

Copyright Warning & Restrictions

The copyright law of the United States (Title 17, United States Code) governs the making of photocopies or other reproductions of copyrighted material.

Under certain conditions specified in the law, libraries and archives are authorized to furnish a photocopy or other reproduction. One of these specified conditions is that the photocopy or reproduction is not to be “used for any purpose other than private study, scholarship, or research.” If a user makes a request for, or later uses, a photocopy or reproduction for purposes in excess of “fair use” that user may be liable for copyright infringement,

This institution reserves the right to refuse to accept a copying order if, in its judgment, fulfillment of the order would involve violation of copyright law.

Please Note: The author retains the copyright while the New Jersey Institute of Technology reserves the right to distribute this thesis or dissertation

Printing note: If you do not wish to print this page, then select “Pages from: first page # to: last page #” on the print dialog screen

The Van Houten library has removed some of the personal information and all signatures from the approval page and biographical sketches of theses and dissertations in order to protect the identity of NJIT graduates and faculty.

**SOLID-LIQUID SUSPENSION IN AGITATED VESSELS
PROVIDED WITH MULTIPLE IMPELLERS**

by
Tong Li

Thesis submitted to the Faculty of the Graduate School of
the New Jersey Institute of Technology
in partial fulfillment of the requirements for the degree of
Master of Science in Chemical Engineering
1991

APPROVAL SHEET

Title of Thesis: Solid-Liquid Suspension in Agitated Vessels
Provided with Multiple Impellers

Name of Candidate: Tong Li

Thesis and Abstract Approved by

Date

Dr. Piero M. Armenante, Associate Professor,
Dept. of Chemical Engineering, Chemistry,
and Environmental Science, NJIT.

Dr. Dana Knox, Associate Professor,
Dept. of Chemical Engineering, Chemistry,
and Environmental Science, NJIT.

Dr. Demetri Petrides, Assisant Professor,
Dept. of Chemical Engineering, Chemistry,
and Environmental Science, NJIT.

VITA

Name: Tong Li

Permanent Address: 1100 Parsippany Blvd., Apt 12
Parsippany, NJ 07054

Degree and date to be conferred: Master of Science in Chemical Engineering, 1991

Collegiate Institutions Attended:	Dates	Degree	Date of Degree
N.J. Institute of Technology	1989-1991	MS	1991
East China Petroleum Institute	1978-1982	BS	1982
Major: Chemical Engineering			

ACKNOWLEDGEMENT

I would like to sincerely acknowledge the guidance and support of my thesis advisor, Dr. Piero M. Armenante. He served as a continuous source of direction and advice. His efforts were truly appreciated.

I would also like to acknowledge the members of my thesis committee, Dr. Dana Knox and Dr. Demetri Petrides, for their support and constructive criticism.

TABLE OF CONTENTS

1.	Introduction	2
2.	Literature Survey	4
2.1	Particle Suspension in an Agitated Liquid	5
2.2	Power Number Theory	7
2.3	Development of Models for Particle Suspension	8
3.	Experimental Apparatus and Method	13
4.	Experimental Procedure	18
5.	Results and Discussion	20
5.1	Effect of Impeller Clearance on N_{js} and P	20
5.1.1	Disc Turbines	20
5.1.2	Flat-Blade Turbines	22
5.1.3	Pitched-Blade Turbines	22
5.2	Effect of Spacing between Impellers on N_{js} and P	23
5.3	Effect of Number of Impellers on N_{js} and P	24
5.4	Effect of Impeller Diameter on N_{js} and P	26
5.5	Power Consumption for Multiple Impeller Systems	28
5.5.1	Effect of Number of Impellers on Power Consumption	28
5.5.2	Effect of Spacing between Impellers on Power Consumption	30
6.	Conclusions	31
	Nomenclature	32
	References	34
	Figures	38
	Appendix - Experimental Data	66

LIST OF FIGURES

1.	Basic Experimental Set-up	38
2.	Wiring Circuits	39
3.	Calibration Curve for Calculation of Power	40
4.	Effect of C on Njs and P (Disc Turbine)	41
5.	Effect of C on Njs and P (Disc Turbine)	42
6.	Effect of C on Njs and P (Flat-Blade Turbine)	43
7.	Effect of C on Njs and P (Flat-Blade Turbine)	44
8.	Effect of C on Njs and P (Flat-Blade Turbine)	45
9.	Effect of C on Njs and P (Pitched-Blade Turbine)	46
10.	Effect of C on Njs and P (Pitched-Blade Turbine)	47
11.	Effect of S on Njs and P (Disc Turbine)	48
12.	Effect of S on Njs and P (Disc Turbine)	49
13.	Effect of S on Njs and P (Disc Turbine)	50
14.	Effect of S on Njs and P (Flat-Blade Turbine)	51
15.	Effect of S on Njs and P (Flat-Blade Turbine)	52
16.	Effect of S on Njs and P (Pitched-Blade Turbine)	53
17.	Effect of S on Njs and P (Pitched-Blade Turbine)	54
18.	Effect of n on Njs and P (Disc Turbine)	55
19.	Effect of n on Njs and P (Disc Turbine)	56
20.	Effect of n on Njs and P (Flat-Blade Turbine)	57
21.	Effect of n on Njs and P (Pitched-Blade Turbine)	58
22.	Effect of D on Njs (Disc Turbine)	59
23.	Effect of D on Njs (Flat-Blade Turbine)	60
24.	Np vs. Re for Multiple Impeller System (Disc Turbine)	61
25.	Np vs. Re for Multiple Impeller System (Disc Turbine)	62

26.	Effect of S on P (Disc Turbine)	63
27.	N_p vs. N for Dual Impeller System (Disc Turbine)	64
28.	N_p vs. N for Dual Impeller System (Disc Turbine)	65

LIST OF TABLES

1.	Effect of Spacing between Impellers on Njs and P	66
2.	Effect of Spacing between Impellers on Njs and P	67
3.	Effect of Spacing between Impellers on Njs and P	68
4.	Effect of Spacing between Impellers on Njs and P	69
5.	Effect of Spacing between Impellers on Njs and P	70
6.	Effect of Spacing between Impellers on Njs and P	71
7.	Effect of Spacing between Impellers on Njs and P	72
8.	Effect of the Number of Impellers on Njs and P	73
9.	Effect of the Number of Impellers on Njs and P	74
10.	Effect of the Number of Impellers on Njs	75
11.	Effect of the Number of Impellers on Njs and P	76
12.	Effect of the Number of Impellers on Njs and P	77
13.	Effect of the Number of Impellers on Njs and P	78
14.	Effect of the Number of Impellers on Njs and P	79
15.	Effect of the Number of Impellers on Njs and P	80
16.	Effect of Spacing between Impellers on P	81
17.	Effect of Spacing between Impellers on P	82
18.	Power Drawn by Each Impeller for Three Impeller System	83

Abstract

A large number of references can be found in the literature on the effect of mixing parameters on the achievement of the minimum agitation speed to just suspend solid particles. In the vast majority of these studies the agitation system consisted of just one centrally mounted impeller. However, the determination of the minimum agitation speed to achieve the just suspended state when the additional impellers are used have received very little attention. It is the intent of this work to investigate the role of multiple impeller agitation system on the achievement of the complete particle suspension state. The effect of a number of variables such as impeller type and size, the impeller clearance off the tank base, the spacing between impellers and the other geometric parameters were studied in detail.

The results obtained here indicate that, contrary to intuition, the presence of the additional impellers may not necessarily be beneficial to the achievement of the just suspended state. In general, it appears that the minimum agitation speed is only slightly affected by the presence of the additional impellers. In particular, if the flow pattern of the additional impellers contrasts with the flow pattern which would be established by a single impeller, then the just suspended state may be achieved at an agitation speed higher for multiple impeller systems than for single impeller systems. Furthermore, the power required to achieve the just suspended state is considerably higher whenever multiple impellers are used. This implies that the bottom impeller is primarily responsible for generating turbulence near the tank bottom (i.e. where the particles become suspended), and for producing particle suspension, independently of the number of impellers used.

Chapter 1

Introduction

Mechanically agitated solid-liquid mixing tanks are widely employed in many chemical and biological processes. These systems typically consist of a mechanically agitated liquid in a stirred tanks, in which solid particles are suspended as a result of agitation. The solid phase may consist of a material undergoing physical or chemical process. Some examples of such systems in chemical and related industries include leaching, dissolution, gas absorption, liquid-liquid extraction and others. Various ore-processing industries also employ such mixing systems. In all these cases it is required that the solid particles be completely suspended.

Of particular significance in solid-liquid systems is the achievement of the just suspended state. This point represents an important balance in the maximization of contact between the two phases and the minimization of power input. Below this point, the surface area of solids is not entirely available for processing. Beyond this point, however, the return on investment may not be justified [3, 19].

The determination of the minimum agitation conditions to achieve the just suspended state of solid particles in a mechanically agitated liquid in tank reactor is a problem of considerable industrial importance which has been studied in the past by a number of investigators [2, 3, 5, 6, 8, 21]. All these studies have been focused on the study of this problem using agitation systems equipped with only one centrally mounted impeller. By contrast, the most industrial reactors, fermenters are provided with multiple impellers mounted on the same shaft.

Therefore, the objective of this work is to study the role of multiple impeller agitation systems on the attainment of the complete suspension state of solid particles in agitated liquids. A number of mixing parameters such as impeller type, size and position, clearance of the bottom impeller off the tank base, spacing between impellers and other geometric and parameters have been investigated as a part of this study. The power drawn by each impeller was also studied in detail.

Chapter 2

Literature Survey

Mixing refers to the physical process which increases the uniformity and homogeneity of mixtures, in terms of their composition, properties, or temperature. In most chemical industries, however, the term "mixing" refers to the operations which [1]:

1. produce the movement or transfer of materials to or from the surface of particles or phases;
2. bring different components (such as solid-liquid, liquid-liquid, gas-liquid) together to produce chemical reactions;
3. promote heat transfer between the equipment surface and the fluid, or between the suspended particles and the continuous phase.

To produce the movement of particles or fluids in mixing operations, external forces are required to overcome the resisting forces that originate from the inertia of the fluid when there is a change in direction or velocity of motion. The shear forces or viscous drag of the fluid also provide another type of resistance to fluid motion. The external forces are usually provided by a rotating agitator. A number of factors such as type, size and structure of the tanks and impellers, and the physical properties of the fluid to be mixed strongly determine the power requirements.

The most common configuration of a typical mixing apparatus used in chemical industries consists of a tank of height nearly equal to the diameter where only one

impeller is provided. However, the use of mixers characterized by a height-to-diameter ratio greater than unity and equipped with multiple impellers is a well established practice for processes where shear-sensitive or high viscosity materials are treated [20], or where a high surface to volume ratio is required because of heat transfer problems. In spite of this wide application, the investigation of solid suspension with multiple impeller agitation system has received very little attention.

2.1 Particle Suspension in an Agitated Liquid

Many chemical processes involve the suspension of solid particles in agitation vessels. Two main suspension states can be defined, namely, complete suspension in which no particle remains on the tank base for longer than a given period (typically one or two seconds), and homogeneous suspension, in which the particle concentration is uniform throughout the tank [3]. The impeller speed at which complete suspension of solids in a liquid is achieved is of great importance in various processing industries. This is because until such a condition is reached the total surface area is not efficiently utilized for mass transfer. Above this speed, the rate at which processes such as dissolution and ion-exchange proceed increases slowly, while the dissipated power increases remarkably [3].

Generally, two techniques have been employed to determine the complete suspension state, namely visual observation and sampling. Zweitering [2] first studied the just completely suspended state at which no particle was visually observed to remain at rest on the tank base for more than one or two seconds. This criterium requires the observation of the illuminated tank base via a mirror placed directly under the tank. The visual observation technique suggests that the flow near the tank base can be either swirling outwards or inwards. A flow which has a sufficient high

velocity will move particles, in the former case, towards the periphery of the vessel, and in the latter, towards the center [10]. This movement is related to a balance between the drag and lift forces arising from the hydrodynamic regime around the particle, and the gravitational forces associated with it.

Instrumented and sampling techniques have also been reported in the literature. These methods are based on the determination of the impeller speed at which the particle concentration just above the base of the vessel reaches a maximum or shows a discontinuity when plotted against the impeller speed. Bourne and Sharma [5] first showed experimentally that a plot of solid concentration against impeller speed formed a peak which coincided with the visually observed value of minimum agitation speed. A possible explanation of this phenomenon is that, at low impeller speed, the concentration of suspended solids near the tank base is very low since the majority of the particles rest on the tank base. As the impeller speed is increased, the particles are gradually suspended, and the solid concentration just above the base of the vessel increases. Eventually the just suspended state is reached when the source of particles on the tank base is practically exhausted. Further speed increases disperse the particles more uniformly throughout the tank and therefore reduce the local concentration of solid near the tank base. However, a discontinuity in the plot of particle concentration against impeller speed in the form of a sharp decrease in gradient rather than a peak was found by Musil [7]. This phenomenon is probably due to the fact that the flow pattern is normally unsteady and is not accurately known. In addition, it is difficult to insure that the samples obtained by means of a sampling tube or draw-off device are truly representative. In any case, several investigators have shown that the values of the sampling technique coincide with, or are very close to, the value determined by visual observation. Usually, the sampling technique gives complete suspension speeds which are slightly lower than the values obtained by visual observation.

In spite of the labor intensity of the sampling method, this technique is less subjective and has advantages in large scale, closed, industrial reactors and tanks where visual observation cannot be applied.

2.2 Power Number Theory

A number of investigators have reported impeller power characteristics in terms of two dimensionless quantities, the Power Number, N_p , and the Reynolds Number, Re . The use of dimensional analysis for correlating impeller power was initially suggested by White and co-workers [27]. This approach was further developed by Hixson and Luedeke [28] and Rushton et al. [29]. Bates et al. [9] reported a power number relationship using impeller diameter, D , as the reference length. The equation they proposed is

$$N_p = \frac{P}{\rho N^3 D^5} = k \left(\frac{\rho N D^2}{h} \right)^a \left(\frac{N^2 D}{g} \right)^b \left(\frac{T}{D} \right)^c \left(\frac{H}{D} \right)^d \left(\frac{C}{D} \right)^e \left(\frac{\rho}{D} \right)^f \left(\frac{W}{D} \right)^g \left(\frac{L}{D} \right)^h \left(\frac{n_2}{n_1} \right)^i \quad (1)$$

where the dependent variable $P/\rho N^3 D^5$ characterizes the flow pattern, and is called the Power Number, N_p . The first term on the right hand side of the equation is known as the tank Reynolds number, Re , and the second term is known as the Froude number. The Reynolds number describes the hydrodynamic effects in the system. The Froude number accounts for vortexing effects in the system. The remaining terms account for the effect of the vessel geometry and impeller geometry.

Bates et al. [9] also pointed out that Equation (1) should be expended to include baffle number and width, spacing of multiple impellers, and off-center impeller

positioning. All of these additional parameters may be included in a form similar to the geometrical terms of Equation (1) or in the form of a factor as used by Bates et al [9].

Chdacek [12] proposed that the effect of the tank bottom shape should also be included in the above analysis, because the tank bottom shape represents a significant geometrical factor with respect to the recirculation pattern.

However, Equation (1) is seldom used in its full form. For a given geometry in the regime $Re > 2000$, Equation (1) reduces to

$$N_p = \frac{P}{\rho N^3 D^5} = k \quad (2)$$

Therefore, Equation (2) may be used to calculate impeller power input if the power number of the impellers is known.

2.3 Development of Models for Particle Suspension

Because of the complexity of the fluid dynamics in an agitated tank, most of the models developed up to this point have had a large empirical basis.

At present, the most commonly used equation to determine the minimum agitation speed for complete suspension is that of Zwietering [2], which gives the minimum agitation speed in terms of the following equation:

$$N_{js} = \frac{Sv^{0.1} d_p^{0.2} (g\Delta\rho/\rho_i)^{0.45} X^{0.13}}{D^{0.85}}$$

This equation was proposed on the basis of dimensional analysis, and was validated experimentally. Zwietering's extensive experimental work covered a wide range of variables including vessel diameter, impeller diameter and type, particle size,

solid concentration and density, liquid density and viscosity, and impeller clearance off the tank base. However, the dimensionless constant, S , was found to be dependent on the system geometry, and the approach employed does not allow an understanding of the phenomenon of particle suspension. For this reason some more theoretical models have been proposed.

Baldi et al [3] proposed that solid suspension is produced by turbulent eddies having a scale proportional to the particle size. With the energy transferred by the eddies, the particles are lifted to a height off the tank base proportional to the particle size. The expression for the minimum agitation speed that they proposed is

$$N_{js} = \frac{(g\Delta\rho/\rho_l)^{0.5} T d_p^{1/6}}{Z P_0^{1/3} D^{5/3}}$$

This equation shows that the agitation speed at the just completely suspended state, N_{js} , is a function of particle size, liquid and solid density, and tank and impeller size.

Narayanan et al. [11] proposed a theoretical expression for N_{js} based on a balance of the forces, assuming that the forces acting on a single particle consisted of the downward gravity force and the upward drag force due to the vertical component of the fluid velocity. However, the effects of the solid concentration and drag coefficient of the particle were not taken into account in determining the minimum impeller speed.

Kolar [22] considered the derivation of the minimum impeller speed from energy balance, assuming that the mixing energy necessary to suspend a particle was equal to the energy dissipated by the particle moving at its terminal velocity in still

fluid. The weakness of the expression he proposed is due to the failure to consider the difference between the settling velocity of a particle in a turbulent fluid and that in a still fluid.

Another theoretical model for the minimum agitation speed was developed by Wichterle [8] in 1987. The model is based on the comparison of the terminal settling velocity, v_p , and the characteristic velocity, v_b , of the agitated liquid around the particle at the bottom, assuming that the velocity field near the vessel bottom can be considered as a laminar boundary layer. The minimum impeller speed was related to a definite critical value of $B = v_b/v_p$, If B is very high, the particle can be suspended. If B is low, the flow around the particle at the bottom is unable to move it. The final expression for the minimum agitation speed is

$$N_{js} = \left(\frac{B_{js}}{A_{\min}}\right)^{2/3} N_0 d_p$$

where the dimensionless function N_0 is

$$N_0 = \left(\frac{d_p}{18 + 0.6d_p^{3/2}}\right)^{2/3}$$

Musil et al. [7] presented a suspension theory based on the assumption that all energy supplied is available to suspended solid particles, and a loss due to the viscous dissipation has to be taken into account within the descending stream of slurry. Two theoretical expressions were developed:

$$Re_{mc} = k_a \left[Ar Re_p \left(\frac{D}{d_p}\right) \left(\frac{\rho_l}{\rho_m}\right) \left(\frac{T^2 z_0}{d_p^3}\right) c \right]^{1/3} \quad (3)$$

$$Re_{mc} = k_b \left[Ar Re_p \left(\frac{D}{d_p}\right) \left(\frac{\rho_l}{\rho_m}\right) \left(\frac{T^2 z_0}{d_p^3}\right) c \right]^{1/3} \left(\frac{CD^2}{T^3} + k_b'\right) \quad (4)$$

where: Re_{mc} is the critical Reynolds number for mixing defined as:

$$Re_{mc} = \frac{N_{js} D^2 \rho_l}{\mu^2}$$

k_a , k_b and k_b' are a dimensionless constant.

Re_p is the particle Reynolds number defined as:

$$\text{Re}_p = \frac{d_p u^2 \rho_l}{\mu^2}$$

z_0 is a constant equal to the thickness of the bottom layer where

the solid particles are present

c is the volume fraction of solid particles

u is a time averaged value of the superficial slip velocity

The Archimedes number, Ar , is defined as:

$$\text{Ar} = \frac{d_p^3 g \rho_l \Delta \rho}{\mu^2}$$

Equation (4) is analogous to Equation (3) except for the last term including the impeller clearance C . Both equations give the minimum suspension speed as a function of the physical properties of the mixed slurry as well as of several selected geometrical parameters of the mixing device.

Many other other investigators have presented a variety of correlations. In a paper by Bohnet and Niesmak [17], these authors summarized the equations for calculation of the critical impeller speed (Table 1).

Table 1. Equations for The Calculation of N_{js}

Gates, Morton, Fondy (1976)
$N_{js} = (\phi w'_{ss} D^{1-2.81})^{1/3.75}; \phi = 6.5 * 10^{10}$ (agitation scale 3) w'_{ss} (ft/min)
Hobler, Zablocki (1966)
$N_{js} = 10.325 \left(\frac{\Delta\rho}{\rho_l}\right)^{0.6} \left(\frac{\rho_s}{\rho_l}\right)^{0.17} g^{0.45} \nu^{0.1} d_p^{0.25} \left(\frac{C}{D}\right)^{0.19} \left(\frac{T}{D}\right) D^{0.9} \left(\frac{c_v}{1-c_v}\right)^{0.17}$
Kneule, Weinspach (1967)
$N_{js} = 1.75 \left(\frac{g \Delta\rho}{D \rho_l}\right)^{0.5} \left(\frac{1}{1 + \frac{\rho_l(1-c_v)}{\rho_s c_v}}\right)^{0.25} \left(\frac{T/D}{3.25}\right)^{5/3}$
Kotzek et al. (1969)
$N_{js} = \left(\frac{c_{ps}}{c_p}\right)^{1/3} \left(\frac{\pi H}{4T}\right)^{0.319} \left(\frac{T}{D}\right)^{0.957} \left(\frac{g \Delta\rho}{D \rho_l}\right)^{0.5} \left(\frac{1}{1 + \frac{\rho_l(1-c_v)}{\rho_s c_v}}\right)^{0.175} \left(\frac{d_p}{D}\right)^{0.21}$
Lamade (1977)
$N_{js} = 5.57 \left(\frac{g \Delta\rho}{D \rho_l}\right)^{0.5} \left(\frac{d_p}{D}\right)^{0.21} \left(\frac{1}{1 + \frac{\rho_l(1-c_v)}{\rho_s c_v}}\right)^{0.15} \left(\frac{C}{D}\right)^{0.115} (T/D)^{-1.5}$
Zlokarnik, Judat (1969)
$N_{js} = 7.08 \left(\frac{g \Delta\rho}{D \rho_l}\right)^{0.5} \left(\frac{d_p}{D}\right)^{1/6} \left(\frac{1}{1 + \frac{\rho_l(1-c_v)}{\rho_s c_v}}\right)^{1/6} \text{EXP}\left(\left(\frac{0.58T}{D}\right)^{-2.27}\right)$
Einenkel, Mersmann (1977)
$N_{js} = 24.93 \frac{\nu^{0.0826}}{D^{0.7768}} (g w'_{ss} c_v \frac{\Delta\rho}{\rho_l})^{0.3058} \left(\frac{T/D}{3.175}\right)^{5/3}$

Chapter 3

Experimental Apparatus and Method

A schematic of the basic experimental set-up used in this work is shown in Figure 1. All experimental work was carried out in three open, flat-bottomed cylindrical vessels constructed of perspex or glass for visual observation. Table 2 gives the vessel dimensions in detail. All tanks were equipped with four baffles to avoid vortex formation. The baffles in the tank with diameter of 29.21 cm and constructed of perspex have width equal to 2.86 cm. The others are equal to 2.54 cm. The baffles were spaced 90 degree apart.

Table 2. Vessel Dimensions

Tank #	Diameter (cm)	Liquid Height (cm)	Tank Height (cm)	Baffle Width (cm)	Materials of Construction
1	24.13	30.48	33.0	2.54	Perspex
2	29.21	33.02	38.6	2.86	Perspex
3	29.21	40.64	44.5	2.54	Glass

All experiments were conducted with a 2.0 horsepower variable speed motor (G.K. Heller Corp.) which had maximum speed of 1,800 rpm. The speed and power measurements were taken with a digital multimeter apparatus which gave the speed of rotation in rpm and the power reading in watts.

Three types of impellers having diameter of 7.62 cm and 10.16 cm were used, namely disc turbines, flat-blade turbines and 45° degree pitched-blade turbines.

Depending on the experiment, one, two or three impellers were mounted on the shaft.

The clearance of lowest impeller off the tank bottom, C , and the spacing between impellers, S , were varied during the experiments.

Distilled water was used as the continuous phase. The ratio between liquid height and tank diameter was $H/T=1.13$ for the 29.21cm diameter tank, and $H/T=1.26$ for the 24.13cm diameter tank in all experiments except those in which only power consumption was investigated (in which case the glass tank was filled with normal tap water only and the height-to-diameter ratio was $H/T=1.39$).

Glass beads with an average size of $115 \mu\text{m}$ were used in this work. The shape of the particles was spherical. The particles were sieved using standard screens, and sedimentated with tap water to obtain a closer size distribution which was analyzed under the microscope. The standard screens were used to determine the size of particles. In making an analysis a set of standard screen was arranged serially in a stack, with smallest mesh at the top and the largest at the bottom. The particles were placed on the top of screen and the stack was shaken mechanically for about thirty minutes. The particle size was determined according to which screen they were retained. The mesh sizes corresponding to an average particle size of $115 \mu\text{m}$ are 120 - 140 mesh ($105\text{-}125 \mu\text{m}$).

In order to determine the power consumption drawn by each impeller independently, three strain gages (Measurements Group Co, CEA-06-187UV-350) were carefully attached and equally spaced on an aluminum hollow shaft with dimension of 9.5 mm in O.D. and 1.65 mm in wall thickness. The strain gages were connected with lead wire to a strain gage conditioner and amplifier system (2120A system) through a slip ring (Electro Miniature Corp.) which avoided winding the wire around the shaft.

A data acquisition system (LABTECH NOTEBOOK) was used to analyze the signal from the strain gage conditioner. Basic wiring circuits are shown in Figure 2. To assure the reliability and accuracy of the strain gage system, the system was calibrated statically by applying known torques (by means of weights) to the shaft.

The aluminum hollow shaft was chosen in accordance with the shear module of elasticity of materials so that when a certain torque was applied on the shaft, it could produce the signal which was high enough to be tested.

The excitation level for the strain gage conditioner and amplifier system was one of the important factors that affected the accuracy of measurement. To achieve best stability and lowest noise at the output, it is desirable to use the maximum excitation that the input to each channel can accept. The excitation level in this work was determined according to the manufacturer's recommendation [25] that a proper excitation level is 2 - 5 volts. The multiplier and gain were determined in accordance with the input range of the data acquisition system which had a minimum input range of $\pm 1.25V$. Table 3 lists the working condition of the strain gage conditioner and amplifier system. The basic set-up configuration of data acquisition system are listed in Table 4.

The power drawn by each impeller was determined through a calibration curve (shown in Figure 3) in which the X-axis represents a known torque applied on the shaft, T (actual torque), and the Y-axis represents a reference torque, T', which was calculated as follows [22]

$$\varepsilon = \frac{2V_r}{GF} \left(1 + \frac{R_t}{R_g}\right)$$

where

ε = Strain : Multiply by 10^6 for micro-strain

R_l = Resistance of lead wire (which was almost equal to 0Ω)

R_g = Resistance of strain gage (which was equal to 350Ω)

GF = Gage Factor (which was equal to 2.0)

$$V_r = \left(\frac{V_{out}}{V_{in}}\right)_{strained} - \left(\frac{V_{out}}{V_{in}}\right)_{unstrained}$$

V_{out} is the output of strain gage conditioner (Volts)

V_{in} is the excitation voltage of strain gage conditioner (Volts)

The reference torque can be calculated with the following equation [26]

$$T' = \frac{4G\varepsilon J}{D_o}$$

where G is the shear modulus of elasticity which was equal to $2.76 * 10^{10}$ Pa

J is the polar moment of inertia of the shaft which can be calculated with following equation

$$J = \pi (D_o^4 - D_i^4) / 32$$

D_o is the outside diameter of the shaft

D_i is the inside diameter of the shaft

The power drawn by each impeller is the following

for the lowest impeller, $P_A = 2\pi N T_A$

for the middle impeller, $P_B = 2\pi N(T_B - T_A)$

for the uppermost impeller, $P_C = 2\pi N(T_C - T_B)$

where T_A , T_B , T_C are actual torques corresponding to the strain gages A, B and C shown in Figure 1.

Table 3. Working Condition of Strain Gage Conditioner and Amplifier System

Excitation	Amplifier	Gain	Bridge Configuration
4V	200	2	Half Bridge

Table 4. Setup Configuration for The Data Acquisition System

Number of Channels [1..100]	3
Current Channel [1..10]	1
Channel Type	[Analog Input]
Channel Name	Voltage 1
Interface device	[0: DT2801]
Interface Channel Number [0..15]	0
Input Units	mv
Input Range	[+/-1.25V]
Scale Factor	1000
Offset constant	1
Buffer size	1000
Number of Iterations	1
Number of Stages [1..4]	1
Sampling Rate, sec.	5
Stage Duration, sec. [0..1.0E+9]	150
Start/Stop Method	[Immediate]
Scale Factor	1000
Offset constant	1
Buffer size	1000
Number of Iterations	1
Number of Stages [1..4]	1
Sampling Rate, sec.	5
Stage Duration, sec. [0..1.0E+9]	150

Chapter 4

Experimental Procedure

The vessel was filled with distilled water to the height which was listed in Table 2, and placed on a clear plastic plate supported by a jack which would allow the tank to be moved vertically. A mirror for the visual observation of particle movement at the tank bottom was placed at a 45° angle under the vessel. A 100 watt lamp was mounted beside the tank. The light was directed to the tank bottom for clear observation. The concentration of solid particles was always fixed at 0.5% of the liquid mass. The weighed particles were then placed in the tank.

The stirrer consisted of a shaft with a variable number of identical, evenly spaced impellers (1-3). The shaft was centrally mounted in the tank. Various impeller clearance off the tank bottom (in the range 0.5D - 1.0D) were tested. The spacing between the impellers was varied in the range 0.625D to 2.333D. The minimum spacing between impellers permitted was 6.35 cm because of the presence of the strain gage. The ratios $H/T=1.263$ in the tank having diameter of 24.13 cm, and $H/T=1.13$ in the tank with diameter of 29.21 cm were used in the experiments for the minimum suspension speed and the corresponding power drawn by each impeller. The power drawn by the multiple impeller system was also examined under the condition $H/T=1.39$ in the tank having diameter of 29.21 cm.

Each run always began at low agitation speed. At each agitation speed, the system was allowed approximately 10 to 15 minutes to reach the steady state. The speed was increased after each observation until the point of complete suspension was reached. Careful attention was paid to the location within the tank where the particles became suspended. This often provided information about the flow pattern near the tank

bottom. The definition of minimum suspension speed, N_{js} , was taken as the speed at which no particles were visually observed to remain at rest on the tank bottom for more than one or two seconds. For each minimum suspension speed, the corresponding power drawn by each impeller was taken from the static calibration curve of strain gages. The corresponding power number, N_p , was calculated with the following equation:

$$N_p = P/(\rho N^3 D^5)$$

Some experiments were conducted to exclusively determine the power number with respect to the agitation speed for disc turbines. In this case, the power drawn by each impeller was recorded at each agitation speed regardless of the particle suspension state.

The output signal from the strain gages was measured with no impellers mounted on the shaft before and after each series of runs. In all cases this output was found to be equal to zero.

Chapter 5

Results and Discussion

5.1 Effect of Impeller Clearance on N_{js} and P

The influence of the impeller clearance, C , on the hydrodynamics of agitated vessels and N_{js} was found to be very significant, and to vary depending on the type of impeller. In this work, the effect of the impeller clearance off the tank bottom on N_{js} was examined under the condition of $H/T=1.26$ for the the tank having diameter of 24.13 cm, and $H/T=1.13$ for the tank with diameter of 29.21 cm. Disc turbines, flat turbines and pitched-blade turbines with diameter ranging from 6.35 to 10.16 cm were used. The clearance was varied from $0.5D$ to $1.0D$ for all types of impeller employed.

5.1.1 Disc Turbines

The influence of impeller clearance on N_{js} for the case of disc turbines are shown in Figure 4 and Figure 5.

As the value of C/D was increased, a change in flow pattern below the lowest impeller occurred. At low clearance the flow at the tank base was observed to be swirling outwards, and the particles were suspended through the periphery at a lower impeller speed. Beyond a certain point ($C/T=0.16-0.21$), suspension occurred exclusively around the center of the tank base. For $S/T < 0.32$, this transition region fell approximately in the range $0.16 < C/T < 0.21$ which was almost the same as that for the case in which only one impeller was used. However, the presence of additional impellers moved this transition region up to the range $0.21 < C/T < 0.26$ when $S/T > 0.35$ as shown in Figure 4(b) through Figure 4(d). A similar behavior was previously reported by Susanto[18] and DeRitter [19] for the single impeller systems. They found that, at $C/T=0.17$, suspension originated at the periphery of the vessel. At $C/T > 0.21$, suspension occurred from the center of the vessel. In the range

$0.17 < C/T < 0.21$, they found that the flow pattern near the tank base became unstable, and the particles were suspended from both the center and the periphery of the vessel. However, for the case in which more than one impeller was used, the transition region was found in our work to be affected by a number of geometrical parameters. This difference can probably be attributed to the fact that at low value of S/D , the two impellers interact heavily. The direction of flow circulation could be changed either from swirling outward to swirling inward or the other way around, depending on the value of S/D and C/D .

The sharp change in the minimum suspension speed as a function of C/D is mainly determined by the change in flow pattern below the lowest impeller which produces a suction effect with consequent formation of vortices. Therefore, the flow characteristics near the tank base were primarily dominated by the lowest impeller on the shaft.

Figure 4 and Figure 5 show the impact of the clearance of the bottom impeller off the tank base on the power drawn by each impeller in the presence of additional impellers. One can see that a significant change in the power drawn by each impeller always corresponds to a region where a transition in flow pattern occurred. In addition, the total power consumption is more sensitive to the impeller clearance than the minimum suspension speed. Therefore, in the presence of multiple impellers, the total power consumption increased more significantly as the impeller clearance was increased.

5.1.2 Flat-Blade Turbines

For this type of impeller, the flow pattern variations were similar to those observed for the case of disc turbines (Figure 6 through Figure 8). The transition region also consisted of an unstable swirling flow pattern. It appears that the range of the transition region is not affected by the presence of additional impellers. This transition region seems always to be in the range $0.666 < C/D < 0.833$. For the case in which only one impeller was employed, no rapid increment of speed was required to achieve the just suspended condition when the transition of flow pattern occurred, as shown in Figure 8(a). However, for the case in which more than one impeller was used, a significant change in N_{js} was observed as C/T increased. It appears that little difference in the range of transition regions exists between the multiple impeller system and the single impeller system. In addition, this behavior seems independent of the spacing between impellers and the number of impellers.

The effect of impeller clearance on the power drawn by each impeller is shown in Figure 6 through Figure 8. The behavior of power consumption is similar to that for the case in which disc turbine were used. A significant change in power consumption also corresponds to the region where a transition in flow pattern occurred. However, for the case in which only one impeller was used, the dependence of the power consumption on C appears to be quite linear, as shown in Figure 8(a).

5.1.3 Pitched-Blade Turbines

For this type of impeller, the direction of rotation was chosen to pump the fluid downward so that the liquid would be pumped toward the resting solids. The opposite

direction of rotation is unsuitable as well as uneconomical for solid suspension. The plot of N_{js} as a function of C/D for pitched-blade turbines pumping downwards are shown in Figure 9 and Figure 10. It can be seen that no transition of flow pattern occurred in the range examined. The flow near the tank base always swirled outwards, and thus the particles were always suspended through the periphery of the vessel. Compared with the other two types of impeller, the pitched-blade turbine requires lower speed to reach the complete suspension state.

Plots of the power drawn by each impeller as a function of C/D are shown in Figure 9 and Figure 10. It appears that the dependence of the power drawn by each impeller on C/D is quite complicated in the presence of multiple impellers. In general, the total power consumption always increases with increasing impeller clearance.

Up to this point, the behavior of multiple impeller systems is very similar to that of single impeller systems although the transition region is somewhat different for the case in which disc turbines or flat turbine are used. These results seem to justify the conclusion that the achievement of the minimum agitation speed for the solid suspension is primarily dominated by the lowest impeller.

5.2 Effect of Spacing between Impellers on N_{js} and P

This study shows that the minimum suspension speed, N_{js} , depends upon the spacing between impellers, S , for the disc turbine. However, little effect of S on N_{js} has been found for flat-blade and pitched-blade turbines. Typical values of N_{js} have been plotted against the spacing between impellers as shown in Figure 11 through Figure 17.

The results indicate that the behavior of dual impeller systems is much more complex than that of single impeller systems. For the case in which disc turbines were used, a transition in flow pattern was observed as the spacing between impellers increased to a critical value which depended on the system examined. This transition was observed only for low values (< 5.08 cm) of the bottom impeller clearance off the tank base, as shown in Figure 11(a), Figure 12(a) and Figure 13(a), (b). Beyond the transition region, the spacing between impellers had little effect on the minimum suspension speed or slightly increased minimum suspension speed as shown in Figure 11(b), Figure 12(b) and Figure 13(c). For the other types of impeller, an increase in the spacing between impeller always involved a slight increase in minimum suspension speed, as shown in Figure 14 through Figure 17.

In general, the spacing between impellers, S , has an effect on the minimum suspension speed, but not as pronounced as the other parameters such as the impeller type or impeller clearance. In some cases, the dependence of N_{js} on S appears to be quite linear as shown in Figure 11(b), Figure 12(b) and Figure 13(c). However, the power consumption increases more sharply. It should be noticed that the power drawn by the two impellers is quite different. The lower impeller consumes less power in most cases.

5.3 Effect of Number of Impellers on N_{js} and P

In order to determine the effect of the presence of additional impellers on the achievement of the minimum agitation speed for solid suspension, a number of experiments were conducted in which N_{js} was determined with 1, 2 and 3 impellers on

the same shaft, and S/D was kept constant at 1. The value C/D varied in the range 0.5 - 1.0.

For the case in which disc turbines were used, at low value of C/T (<0.17), the minimum suspension speed was not significantly affected by the presence of additional impellers as shown in Figure 18(a), (b) and Figure (19(a). Beyond this point ($C/T > 0.17$), the minimum suspension speed was reduced by the addition of the second impeller. However, little further improvement on the minimum suspension speed was observed in the presence of the third impeller, as shown in Figures 18(c), (d) and 19(b).

The results obtained for flat turbines indicate that when $C/D < 0.67$, the presence of a second impeller has little effect on the minimum suspension speed requirement. However, the addition of the third impeller involves an increase in the minimum suspension speed requirements, as shown in Figure 20(a). When $C/D > 0.67$, the addition of second impeller causes an increase of the minimum suspension speed. However, the minimum suspension speed was reduced by the addition of a third impeller, as shown in Figure 20(b), (c).

For pitched turbines, the minimum suspension speed either slightly increased or was not affected by the presence of any additional impellers, as shown in Figure 21. This behavior seems independent of the value of C/D and S/D .

Therefore, contrary to intuition, the presence of multiple impellers may not necessarily be beneficial to the achievement of the minimum suspension speed. In particular, if the flow pattern of the additional impellers contrasts with the flow pattern which would be established by a single impeller, then the just suspended state may be

achieved at a agitation speed higher for multiple impeller systems than for the corresponding single impeller system.

Since the flow pattern around the impellers and the turbulence caused by each impeller affect the achievement of the just completely suspended state, the difference in flow pattern around the bottom impeller is probably the reason behind these results. Further studies are expected to give a better explanation on this behavior.

As for the achievement of the minimum agitation speed for solid suspension, the power required to achieve the just completely suspended state is considerably higher when multiple impellers are used. Furthermore, the presence of additional impellers may even require a higher speed to achieve the just completely suspended state. In the majority of cases the presence of the additional impellers increases the power supplied to the fluid without improving the achievement of the just completely suspended state, as shown in Figure 18 through Figure 21. This means that an increase in the power dissipated by additional impellers does not involve a decrease in the minimum suspension speed, since the complete suspension state depends on the degree of turbulence near the tank base which is primarily dominated by the lowest impeller.

5.4 Effect of Impeller Diameter on N_{js} and P

In this work, the effect of impeller diameter was examined in two different ways:

- (1) The value of C/D was kept constant as the impeller size was varied;
- (2) The value of C was kept constant as the impeller size was varied.

The first procedure was previously employed by both Baldi et al. [3] and Susanto [18] in systems provided with only one impeller. Zwietering [2] and Chapman [23] employed the second approach, and also used only one impeller.

Both conditions were tested with the same type of turbines for three different sizes (6.35, 7.62, and 10.16 cm) in the same tank (T=29.21cm). The plots of N_{js} vs. D on a log-log scale are shown in Figure 22 and Figure 23:

For C=5.08 cm, the results give

$$N_{js} \propto D^{-2.25} \quad \text{for } n=1 \text{ disc turbine}$$

$$N_{js} \propto D^{-2.12} \quad \text{for } n=2 \text{ disc turbines}$$

$$N_{js} \propto D^{-2.15} \quad \text{for } n=3 \text{ disc turbines}$$

$$N_{js} \propto D^{-1.97} \quad \text{for } n=2 \text{ flat turbines}$$

For C/D=constant, the relationships are:

$$N_{js} \propto D^{-1.78} \quad \text{for } n=1 \text{ disc turbine at } C/D=0.5$$

$$N_{js} \propto D^{-1.74} \quad \text{for } n=2 \text{ disc turbines at } C/D=0.5$$

$$N_{js} \propto D^{-1.75} \quad \text{for } n=3 \text{ disc turbines at } C/D=0.5$$

$$N_{js} \propto D^{-2.31} \quad \text{for } n=1 \text{ disc turbine at } C/D=1.0$$

$$N_{js} \propto D^{-1.70} \quad \text{for } n=2 \text{ disc turbines at } C/D=1.0$$

$$N_{js} \propto D^{-1.71} \quad \text{for } n=1 \text{ flat turbine at } C/D=0.5$$

$$N_{js} \propto D^{-1.64} \quad \text{for } n=2 \text{ flat turbines at } C/D=0.5$$

The exponents found here compare well with those obtained by previous investigators for system provided with only one impeller on the shaft. Baldi et al. [3] found that for an eight blade disc turbine

$$N_{js} \propto D^{-1.67} \quad \text{at } C/D=0.5$$

$$N_{js} \propto D^{-1.89} \quad \text{at } C/D=1.0$$

DeRitter [19] found that for a six blade disc turbine it is:

$$N_{js} \propto D^{-1.695} \quad \text{at } C/D=0.5$$

$$N_{js} \propto D^{-1.918} \quad \text{at } C/D=1.0$$

Similarly, Zwietering's [2] data concerning the effect of impeller diameter for disc turbine resulted in:

$$N_{js} \propto D^{-2.35} \quad \text{for constant } C$$

whereas Chapman et al. [23] reported the following relationship

$$N_{js} \propto D^{-2.45} \quad \text{for constant } C$$

Nienow's data [6] were correlated by

$$N_{js} \propto D^{-2.21} \quad \text{for disc turbine at constant } C$$

These results are in close agreement with those found in this works. This seems to reinforce the concept presented above, that the difference between single impeller systems and multiple impeller systems is not very significant.

5.5 Power Consumption for Multiple Impeller Systems

The power dissipated by multiple impeller systems was examined in the vessel with $T = 29.21$ cm and $H = 1.39T$. Disc turbines having 7.62 cm and 10.16 cm diameter were used. Depending on the experiment one, two or three impellers were mounted on the shaft. The values S/D and C/D were always equal to 1 for the case in which three impellers were used. For the two impeller system, the value S/D was varied during the experiment, but C/D was kept constant at 1.

5.5.1 Effect of Number of Impellers on Power Consumption

For a single impeller system, the average power number over a range of $Re = 34,000 - 83,000$ is 4.5 for disc turbine. This value is almost the same as that previously reported by Lu et al.[14]. Under the condition of $D/T = 0.35$, the measured total power number for two- and three-impeller systems is 7.5 and 10.1

respectively, as shown in Figure 24. It appears that the power dissipated with more than one impellers is not entirely proportional to the number of impellers employed.

The results obtained for the three impeller system are shown in Figure 24(b) and Figure 25(b). It appears that the total power dissipated by three impellers is not equally distributed among the three impellers. In the range $Re > 25,000$ and $D/T = 0.35$, the top impeller had an average power number of 3.6. The power number of the bottom impeller had an average value of 3.4, while the middle impeller had the lowest average power number of 2.3. A similar behavior was also observed under the condition of $D/T = 0.26$, as shown in Figure 25(b). In general, the power drawn by each impeller out of total power consumption is about 38% for the top impeller, 26% for the middle impeller and 36% for the lowest impeller respectively.

This behavior seems to be independent of the value of D/T . The possible explanation for this behavior could be the following. For the case in which three impellers are used under the condition of $S/D = 1$, the top impeller will agitate a liquid region bordering the gas-liquid interface, while the bottom impeller will move a liquid region bordering the interface between the liquid and solid tank base. The middle impeller will move the liquid contained in a region bordering the homogeneous liquid interfaces which have already been moved by the other impellers in the same direction of impeller rotation. Compared with the resistance of gas-liquid or solid-liquid interface, the resistance to be overcome by the middle impeller would be obviously smaller. Therefore, the power drawn by the middle impeller would be the least. Similarly, the resistance offered by the gas-liquid interface would be smaller than that of the solid-liquid interface. This could be the reason that power consumption for the top impeller is smaller than that for the bottom impeller.

5.5.2 Effect of Spacing between Impellers on Power Consumption

The spacing between impellers significantly affects the behavior of the two impeller systems. The results shown in Figure 26 are somewhat similar to those presented by Hudcova et al. [15]. For spacing in the range $0.6 < S/D < 1.2$, the power consumption slightly increased with increasing S . As stated by Chiampo et al.[13] the only outcome of increasing S that can be detected is a growth of the amount of liquid between two impellers. Therefore, a very moderate increase of the power drawn in this range can be observed. For $S/D > 1.2$, a steep increase of the power drawn can be observed when S increased. A possible explanation is that since the dependence of the power drawn by each impeller on spacing between impellers is closely linked to the bulk flow pattern, a sharp change in power consumption is probably caused by a change in degree of turbulence between impellers. As stated by Hudcova et al.[15] for $S/D > 2$ the power drawn by the two impeller system is approximately twice that of a single impeller. However, as previously observed by Chiampo et al.[13] the value of 2 for the ratio of the power dissipated by the dual impeller system to the power drawn by the single impeller system can be measured at impeller spacing less than 2, as shown in Figure 28(c).

The average value of power drawn by the each impeller out of total power consumption is about 54% for the upper impeller, and 46% for the lower one in the range $0.6 < S/D < 1.2$. Kuboi and Nienow [24] have conducted similar studies with two Rushton type impellers in a standard vessel $H=T$, and have determined each of their contributions to the total power. They have already confirmed that, in general, the upper impeller would draw more power than the lower one.

Chapter 6

Conclusions

1. Multiple impeller configurations may not necessarily be beneficial to the achievement of the just completely suspended state in solid-liquid systems. In the majority of cases, it appears that the presence of additional impellers does not significantly improve the achievement of the minimum suspension speed. In particular, if the flow pattern of the additional impellers contrast with the flow pattern which would be established by a single impeller then the just suspended state may be achieved at agitation speeds higher for multiple impeller configurations than for a single impeller system. An increase in the power dissipated by additional impellers does not involve a decrease in the minimum suspension speed, since the complete suspension state depends on the degree of turbulence near the tank base, which is primarily dominated by the lowest impeller on the shaft.

2. For multiple impeller configurations, the power dissipated is not entirely proportional to the number of impellers used. For a three-impeller system, it was found that the power drawn by each impeller is different. Under the condition of $S/D=1$ and $C/D=1$, the average power numbers for disc turbine in the range $Re > 25,000$ are 3.6 for the bottom impeller, 2.3 for the middle impeller and 3.4 for the top impeller respectively. For a two-impeller system, it is found that, in general, the upper impeller would drawn more power than the lower one. In the range $0.6 < S/D < 1.2$, the average value of power drawn by the each impeller out of total power consumption is about 54% for the upper impeller and 46% for the lower one.

Nomenclature

A	Normalized shear rate
A_{\min}	Minimum value of A
Ar	Archimides number (nondimensional) $\frac{d_p^3 g \rho_l \Delta \rho}{\mu^2}$
c	Volume fraction of solid particles
C	Impeller clearance of the lowest impeller measured from the tank base (cm)
c_p	Power coefficient
c_{ps}	Suspension coefficient
c_v	Effective solids hold-up, (m^3/m^3)
d_p	Diameter of solid particle (μm)
D	Impeller diameter (cm)
D_o	Outside diameter of the shaft (cm)
D_i	Inside diameter of the shaft (cm)
Fr	Froude number (nondimensional) $\frac{N^2 D}{g}$
g	Acceleration due to gravity (m/sec^2)
G	Shear modulus of elasticity (Pa)
GF	Gage Factor (nondimensional)
H	Liquid height (cm)
J	Polar moment of inertia of the shaft ($J = \pi(D_o^4 - D_i^4)/32$)
n	Number of impellers
N	Impeller speed (rpm)
N_{is}	Minimum speed required to "just suspend" the solid phase (rpm)
N_p	Power number, $P/(\rho N^3 D^5)$ (nondimensional)
P	Power input (watts)
P_A	Power drawn by Impeller A (watts)

P_B	Power drawn by Impeller B (watts)
P_C	Power drawn by Impeller C (watts)
P_T	Total Power Consumption (watts)
Re	Reynolds number, $\rho ND^2/\mu$ (nondimensional)
Re_{mc}	Critical Reynolds number for mixing, $\frac{N_{js} D^2 \rho_1}{\mu^2}$ (nondimensional)
Re_p	Particle Reynolds number, $\frac{d_p u^2 \rho_1}{\mu^2}$ (nondimensional)
R	Resistance of lead wire (Ω)
R_g	Resistance of strain gage (Ω)
S	Spacing between impellers (cm)
T	Tank diameter (cm)
T'	Reference torque ($\frac{4G\epsilon J}{D_a}$)
T_A	Actual torque corresponding to the strain gage A
T_B	Actual torque corresponding to the strain gage B
T_C	Actual torque corresponding to the strain gage C
V_{out}	Output of strain gage conditioner (Volts)
V_{in}	Excitation voltage of strain gage conditioner (Volts)
v_b	Characteristic velocity of the agitated liquid around the particle
v_p	Terminal settling velocity of particle
w_{ss}	Terminal settling velocity, (m/s)

Greek Symbols

λ	Size of a turbulent eddy (m)
ϵ	Strain, multiply by 10^6 for micro-strain
ν	Kinematic viscosity (m^2/s)
μ	Dynamic viscosity (cp)

ρ_l	Liquid density (kg/m ³)
ρ_m	Mean density of mixed slurry (kg/m ³)
ρ_s	Solid density (kg/m ³)
$\Delta\rho$	Difference between solid density and liquid density, $\rho_s - \rho_l$ (kg/m ³)
ϕ	Stirring function

References

1. Oldshue, J. Y., "*Fluid Mixing Technology*". McGraw-Hill Publications Co., New York, NY (1985)
2. Zwietering, T. N.; "Suspending of Solid Particles in Liquid by Agitators", *Chemical Engineering Science* **8**: 244-253 (1958).
3. Baldi, G., Conti, R, Alaria, E.; "Complete suspension of Particles in Mechanically Agitated Vessels", *Chemical Engineering Science*, **33**: 21-25 (1978)
4. Conti, S. S., Specchia, V.; "Effect of The Stirrer Clearance on Particle Suspension in Agitated Vessels", *Chemical Engineering Journal*, **22** :247-249 (1981)
5. Bourne, J. R., Sharma, R. N.; "Homegeneous Particle Suspension in Propeller-Agitated Flat Bottomed Tanks"; *Chemical Engineering Journal*, **8**: 243-250 (1974)
6. Nienow, A. W.; "Suspension of Solid Particles in Turbine Agitated Vessels", *Chemical Engineering Science*, **23**: 1453-1459 (1968)
7. Musil, L., Vlk, J.; "Suspending Solid Particles in An Agitated Conical-Bottom Tank", *Chemical Engineering Science*, **33**: 1123-1131 (1978)
8. Wichterle, K.; "Conditions for Suspension of Solids in Agitated Vessels", *Chemical Engineering Science*, **43**: 467-471 (1988)
9. Bates, R. L., Fondy, P. L. and Corpstein R. R.; *Ind Eng. Chem. Process Design and Development*,**2**:310 (1963)
10. Nienow, A. W.; "*Dispersion of Solid in Liquids*", McGraw Hill Book, New York, NY, page 282 (1987)
11. Narayanan, S., Bhatia, V. K., Guha, D. K. and Rao, M. N.; "Suspension of Solids by Mechanical Agitation", *Chemical Engineering Science*, **24**: 223-230 (1969)

12. Chudacek, M. W.; "Impeller Power Numbers and Impeller Flow Numbers in Profiled Bottom Tanks", *Ind. Eng. Chem. Process Des. Dev.*, **24**: 858-867 (1985)
13. Chiampo, F., Guglielmetti, R., Manna, L. and Conti, R.; "Gas-Liquid Mixing in A Multiple Impellers Stirred Vessel", *Ind. Eng. Chem. Process Des. Dev.*, **24**: 858-867(1985)
14. Lu, W-M. and Yao, C-L., "Gas Dispersion in A Multi-Stage Impeller Stirred Tank"*Proc. 7th Eur. Conf. Mixing*, Brugge, Belgium, Sept. 18 - 20, 1991
15. Hudcova, V., Machon, V. and Nienow A. W.; "Gas-Liquid Dispersion with Dual Rushton Turbine Impellers", *Biotechnology and Bioengineering*, **34**: 617-628 (1989)
16. Roustan, M.; "Power Consumed by Rushton Turbines in Non Standard Vessels under Gassed Conditions", 5th European Conference on Mixing, Wurzburg, West Germany, June 10-12, 1985
17. Bohnet, M. and Niesmak, G.; "Distribution of Solids in Stirred Suspensions", *Ger. Chem. Eng.* **3**: 57-65 (1980)
18. Susanto, J., "Mutiphase Solid-Liquid and Solid-Liquid-Das Mixing in Srrred Tanks", Master's Thesis, New Jersey Institute of Technology (1989).
19. DeRitter, G. R., "Multiphase Solid-Liquid-Liquid Mixing in Stirred Tanks", Master's Thesis, New Jersey Institute of Technology (1990).
20. Fajner, D., Magelli, F. and Pasquali, G.; "Modelling of Nonstandard Mixers Stirred with Multiple Impellers", *Chem. Eng. Commun.*, **17**: 285-295 (1982)
21. Kolar, V.; "Suspending Solid Particles in Liquids by Means of Mechanical Agitation", *Collection Czechoslov. Chem. Commun.*; **26**: 613-627 (1961)
22. Omega Engineering, Inc., Complete Pressure and Strain Measurement Handbook and Encyclopedia.

23. Chapman, C. M., Nienow, A. W., Cooke, M. and Middleton, J. C.; "Particle-Gas-Liquid Mixing in Stirred Vessels. Part 1: Particle-Liquid Mixing", *Chem. Eng. Res. Dev.*, **61**: 71-81 (1983)
24. Kuboi, R., Nienow, A. W., "The Power Drawn by Dual Impeller Systems under Gassed and Ungassed Conditions", Proc. 4th Eur. Conf. Mixing, G2, Noordwijkerhout, Netherlands, BHRA, (1982)
25. Measurements Group, Inc., "Optimizing Strain Gage Excitation Levels", TN-502, Raleigh, North Carolina, U.S.A. (1979)
26. Muvdi, B. B. and McNabb, J. W., "*Engineering Mechanics of Materials*". Springer-Verlag New York Inc., New York, NY (1991)
27. White, A. M. and Brenner, E., "Studies in Agitation, V. The Correlation of Power Data", *Trans American Institute of Chemical Engineers* **30**: 585-597 (1934)
28. Hixson, A. W. and Luedeke, V. C., "Wall Friction in Liquid Agitation System", *Ind. Eng. Chem.*, **29**: 927-933 (1937)
29. Rushton, J. H., Costich, E. W. and Evert, H. J., "Power Characteristics of Mixing Impellers", *Chem. Eng. Prog.*, **46**: 395-404 (1950)

Figure 1. Basic Experimental Set-up

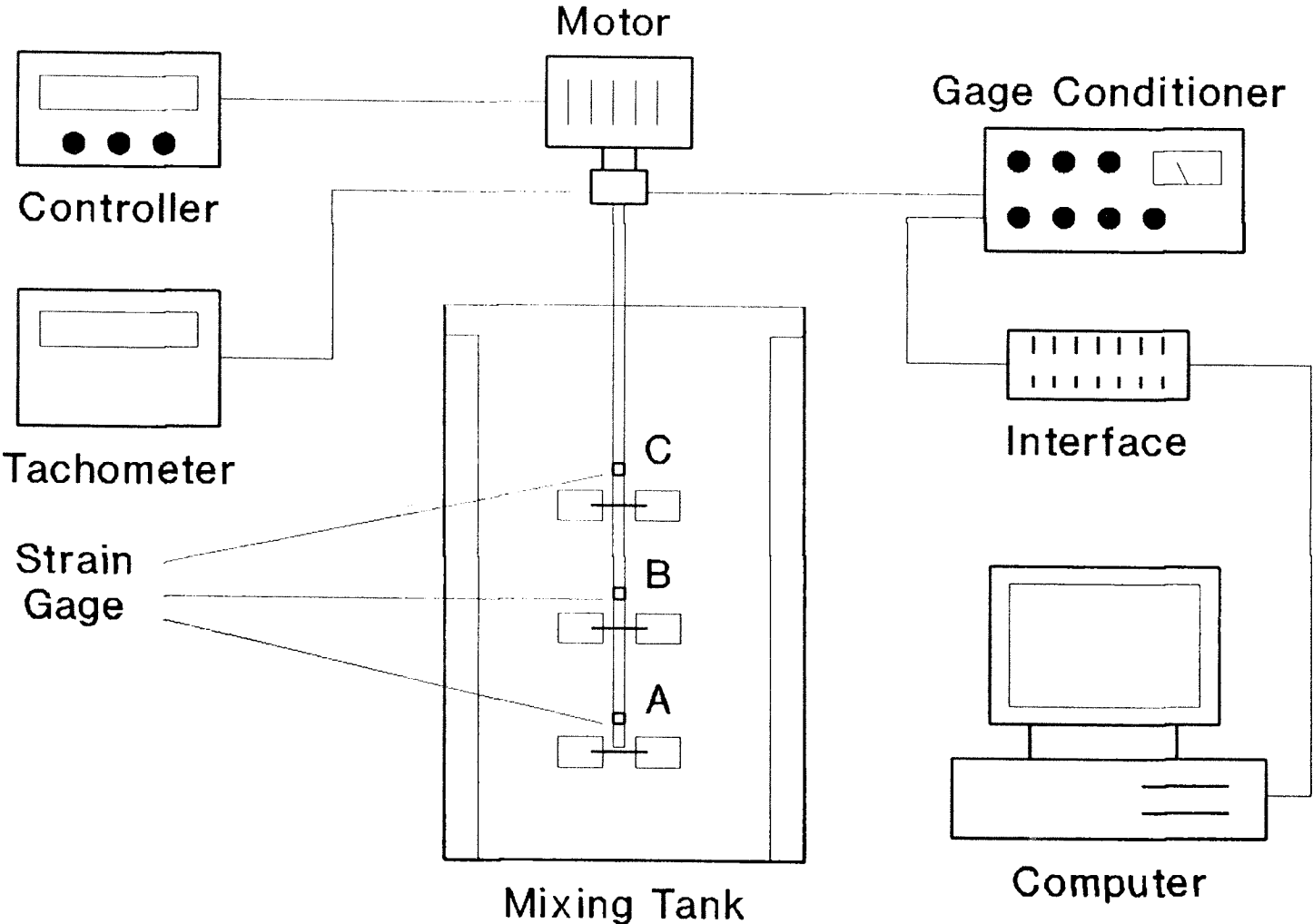
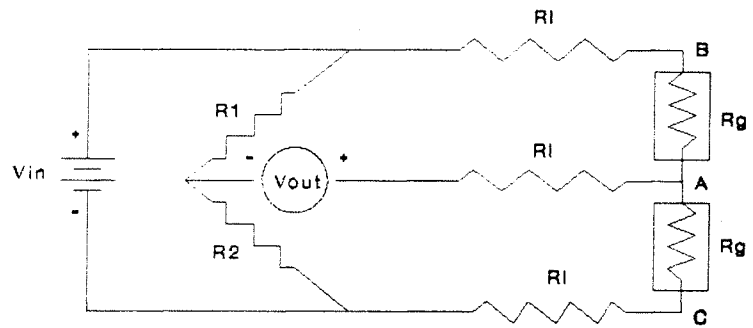
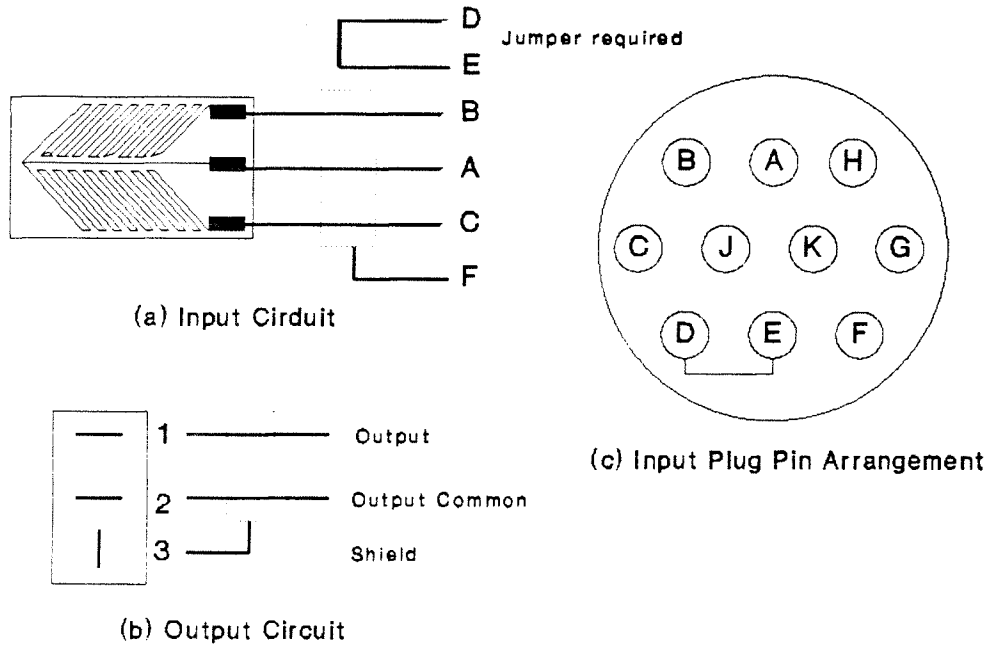


Figure 2. Wiring Circuits



(d) Half Bridge Configuration

Figure 3. Calibration Curve
For Calculation of Power

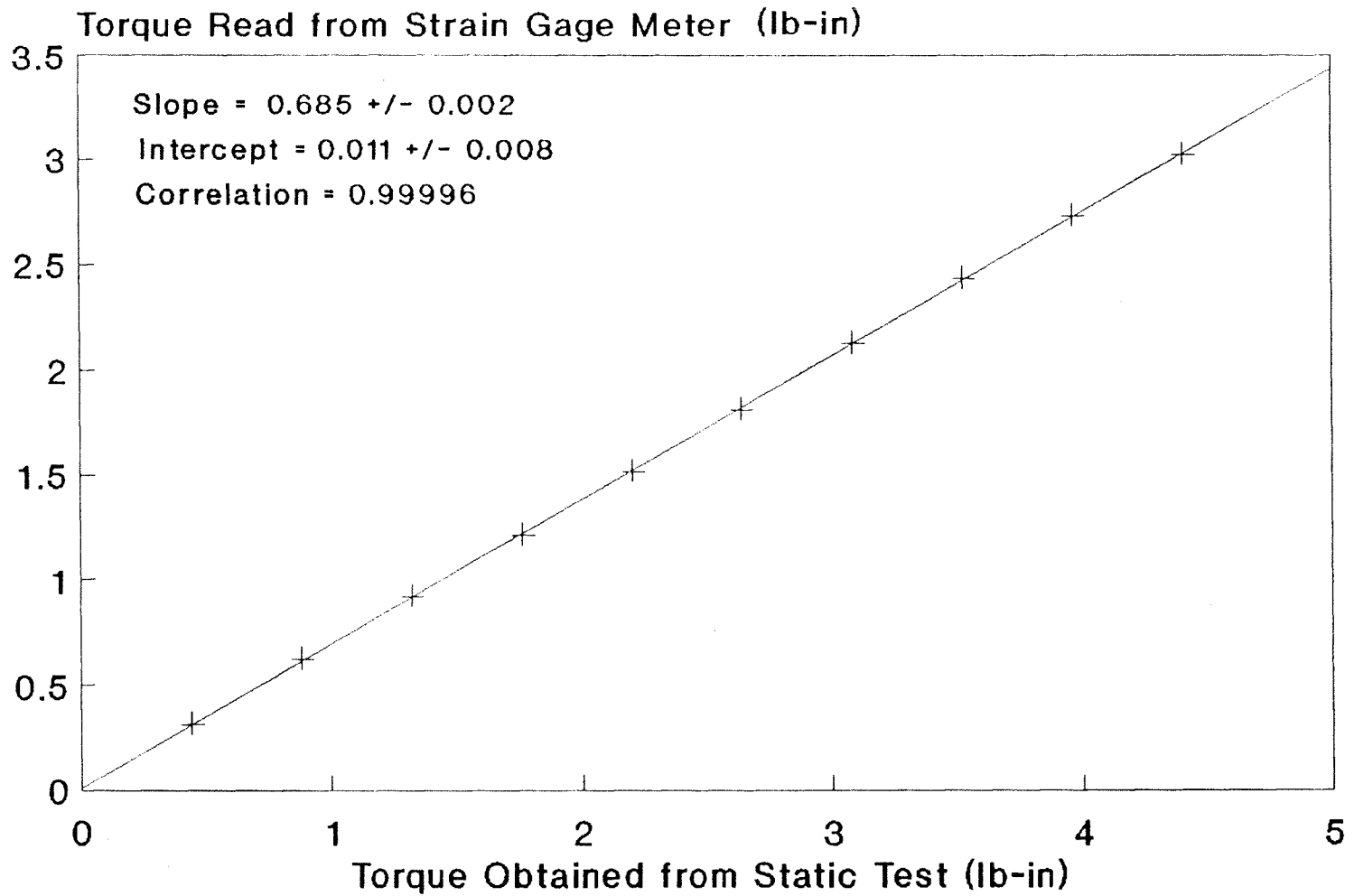
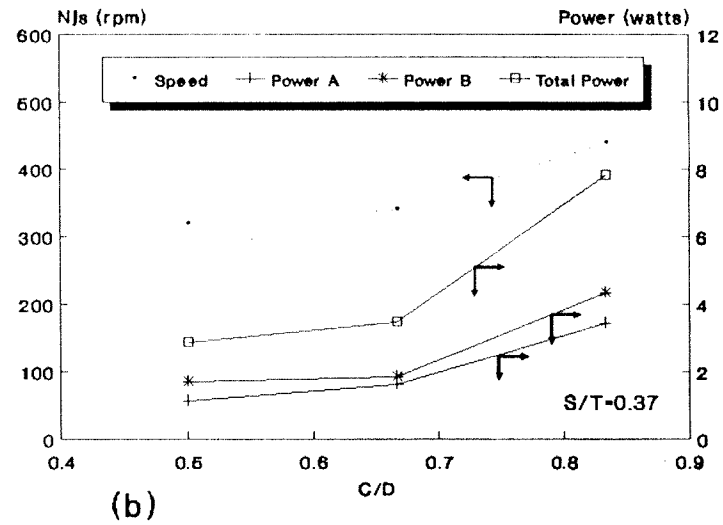
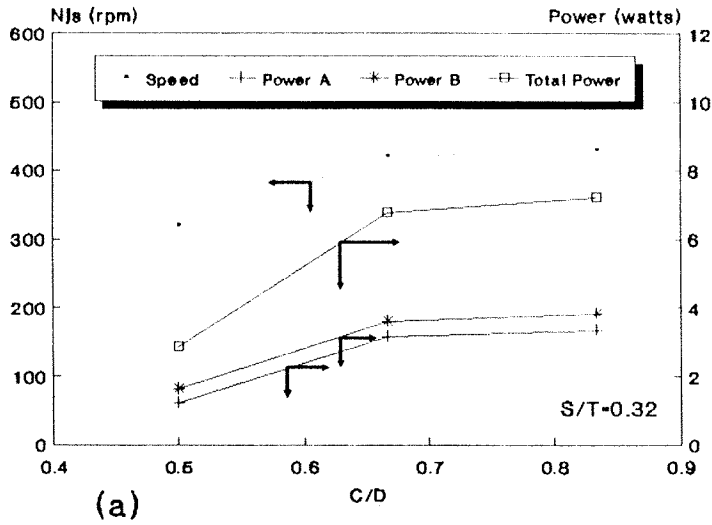
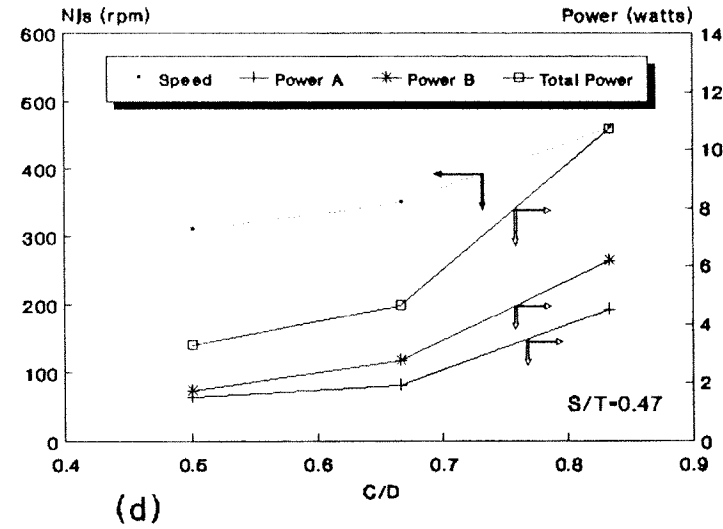
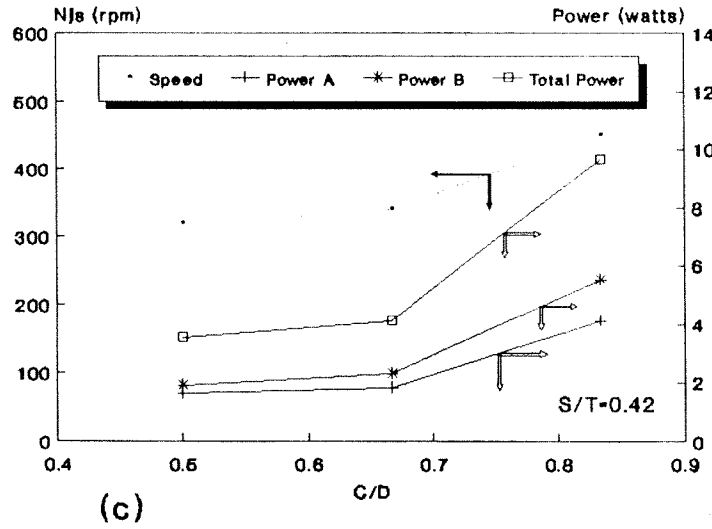
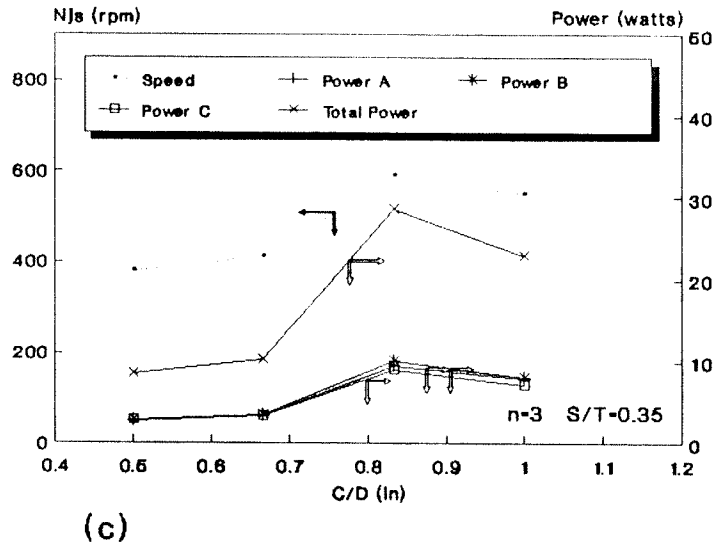
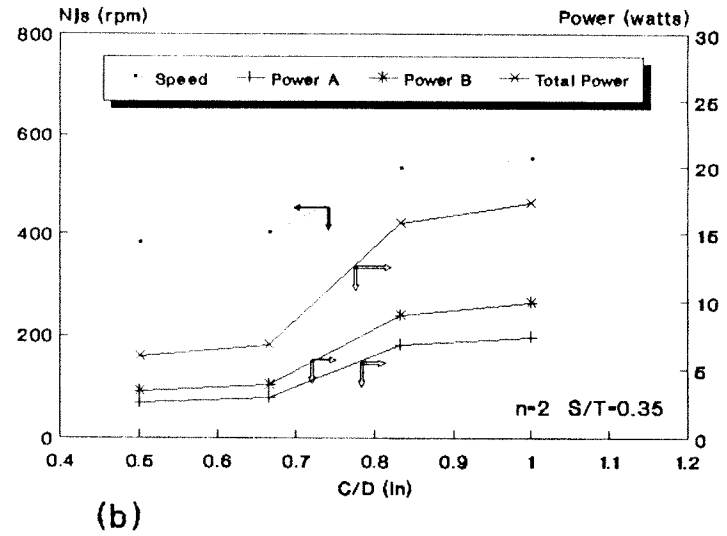
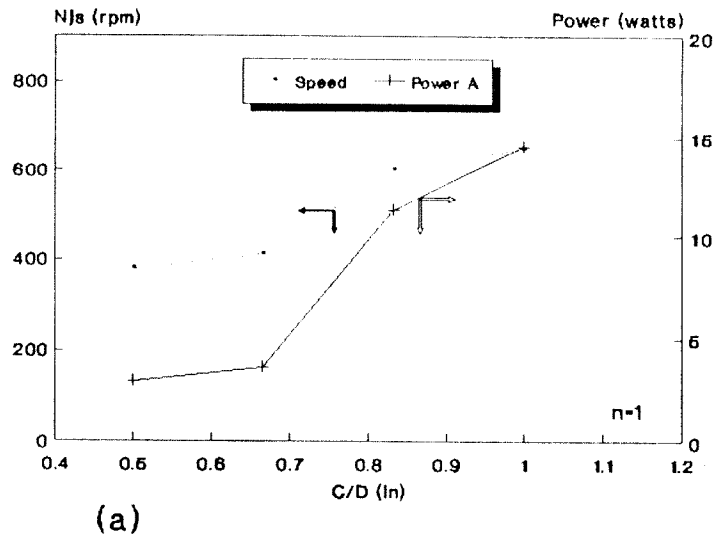


Figure 4. Effect of C on Njs and P



Disc Turbine T=24.13cm H=30.48cm D=7.62cm X=0.5% n=2





Disc Turbine

T=29.21cm

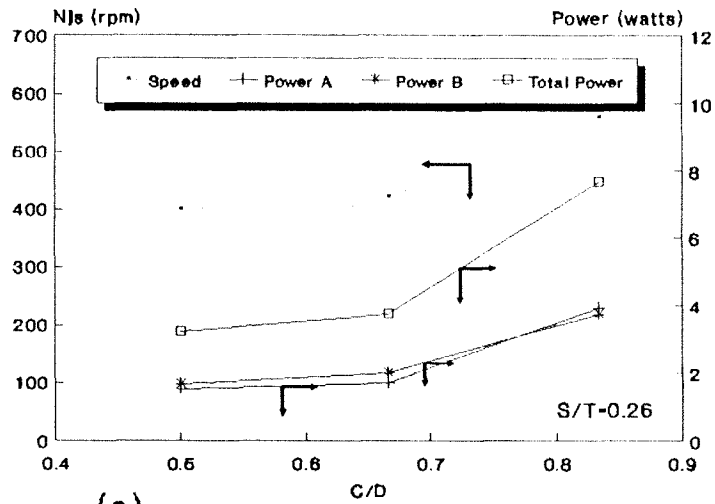
H=33.02cm

D=7.62cm

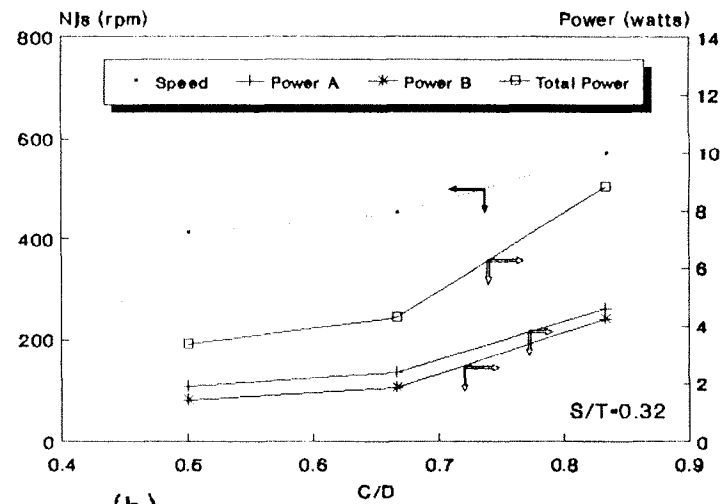
X=0.5%

Figure 5. Effect of C on Njs and P

Figure 6. Effect of C on Njs and P

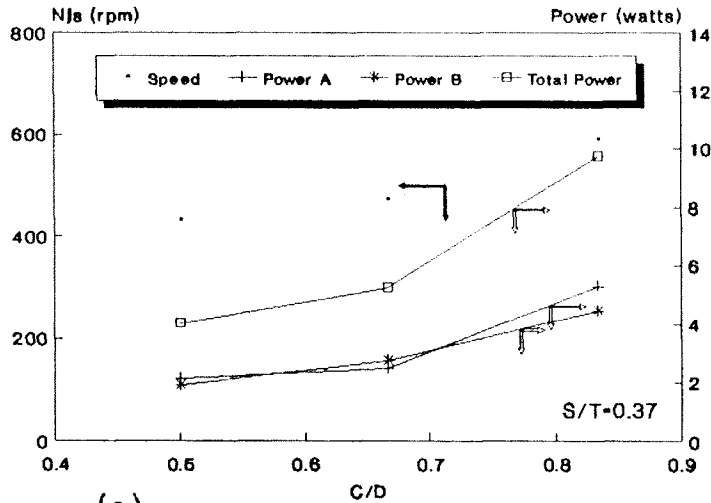


(a)

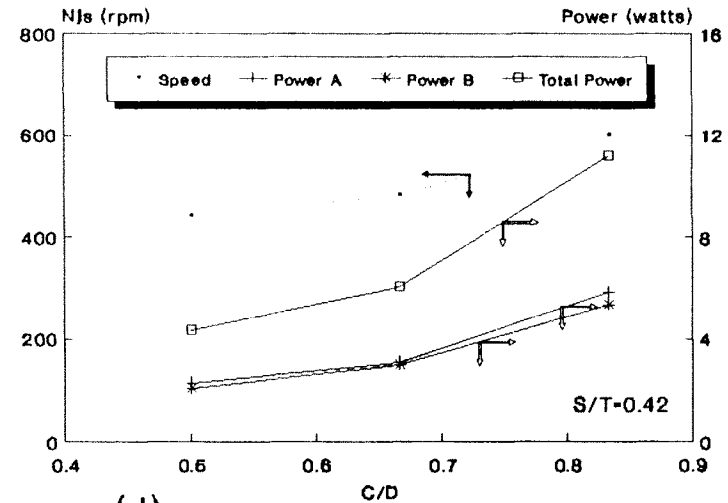


(b)

Flat Turbine T=24.13cm H=30.48cm D=7.62cm X=0.5% n=2

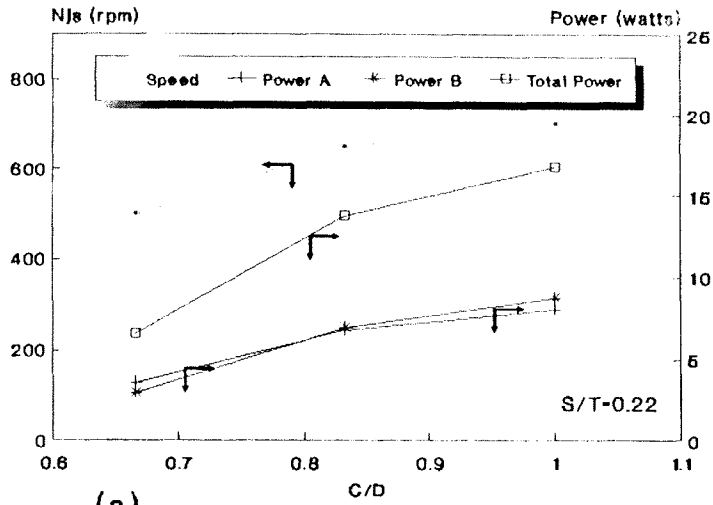


(c)

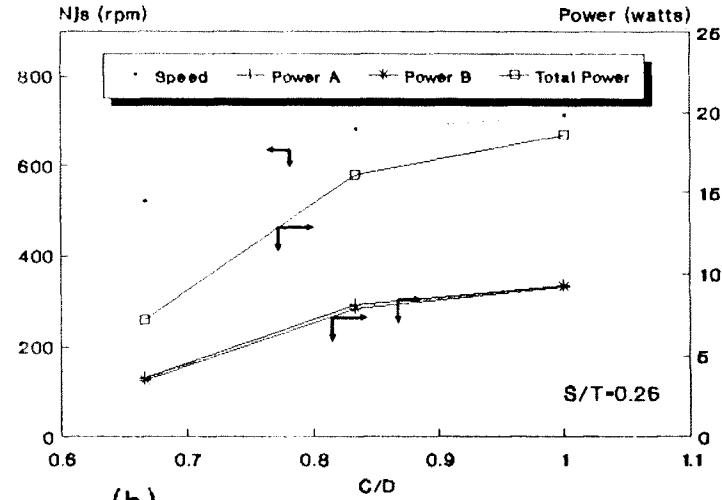


(d)

Figure 7. Effect of C on Njs and P

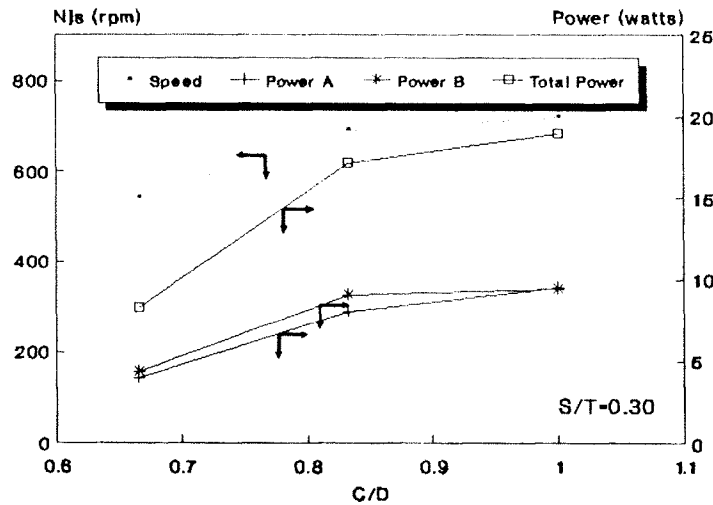


(a)

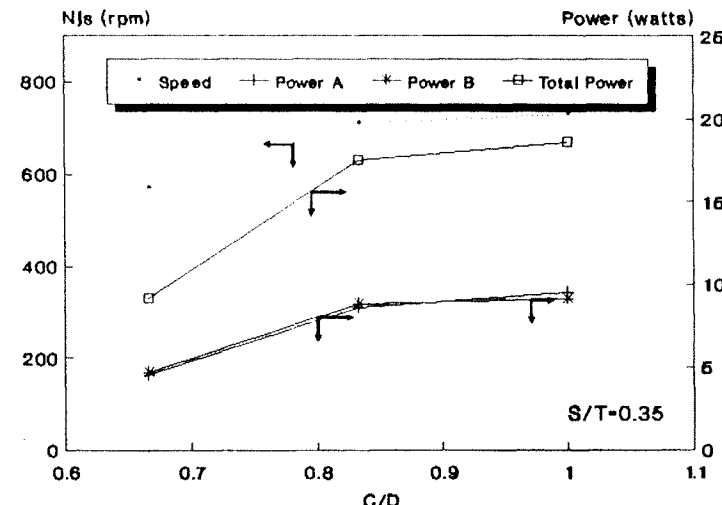


(b)

Flat Turbine T=29.21cm H=33.02cm D=7.62cm X=0.5% n=2

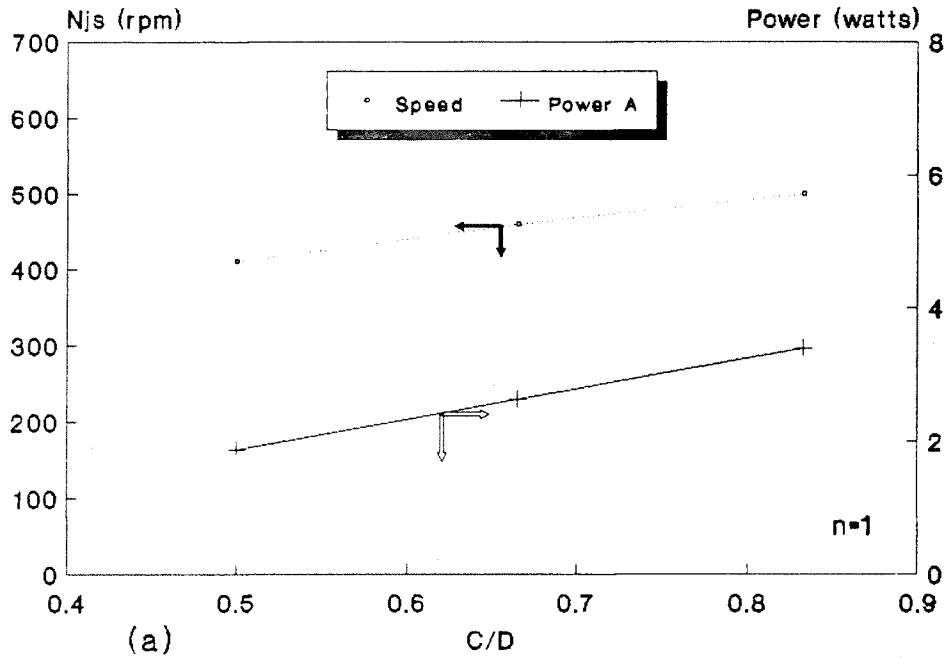


(c)



(d)

Figure 8. Effect of C on Njs and P



Flat Turbine

T=24.13cm H=30.48cm D=7.62cm X=0.5%

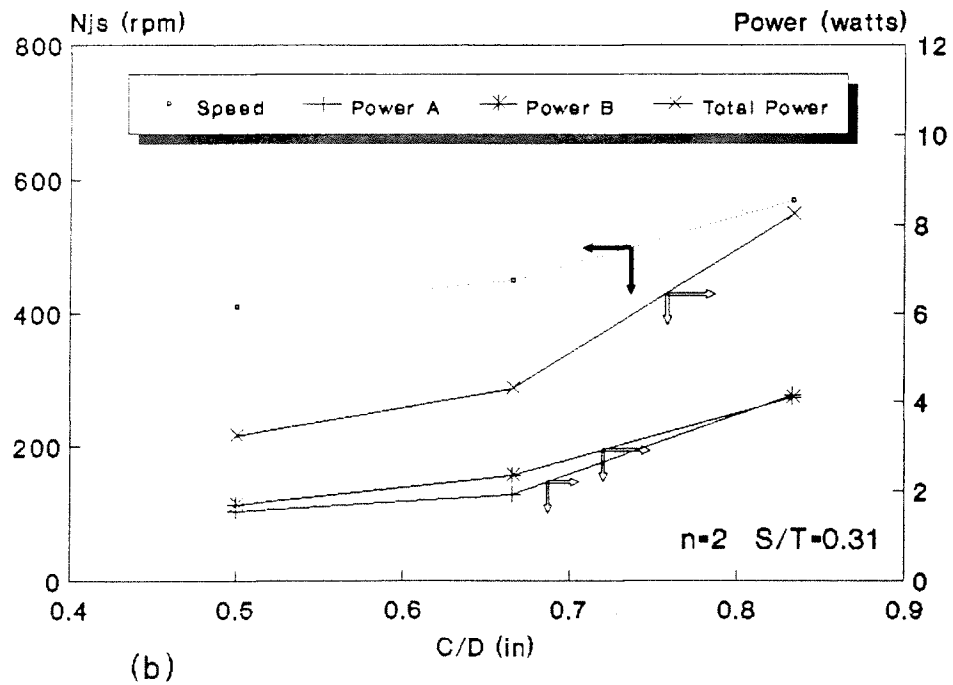
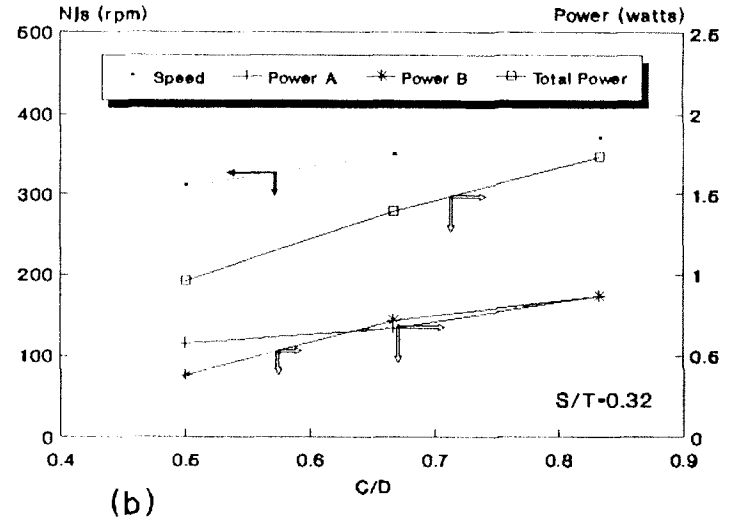
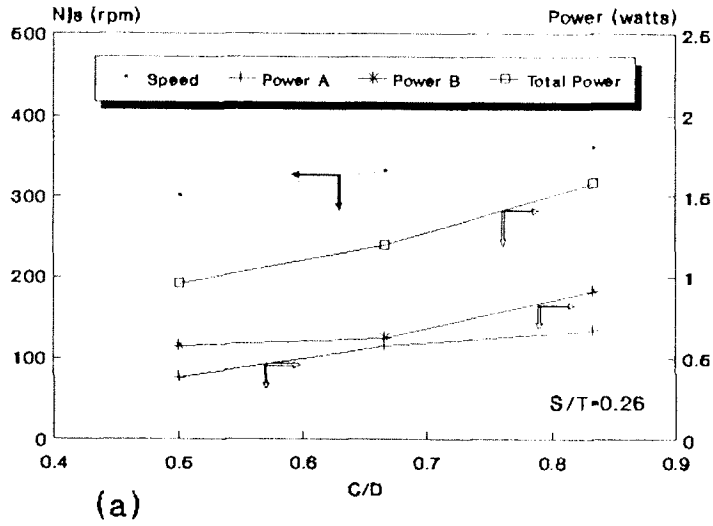


Figure 9. Effect of C on Njs and P



Pitched Turbine T=24.13cm H=30.48cm D=7.62cm X=0.5% n=2

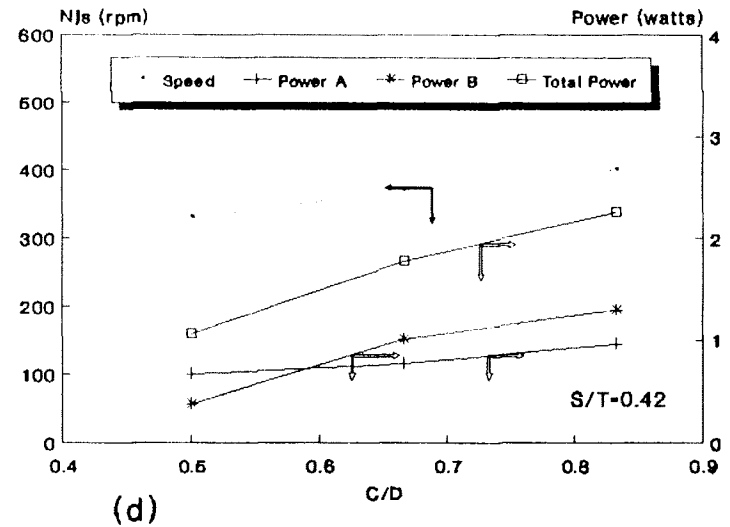
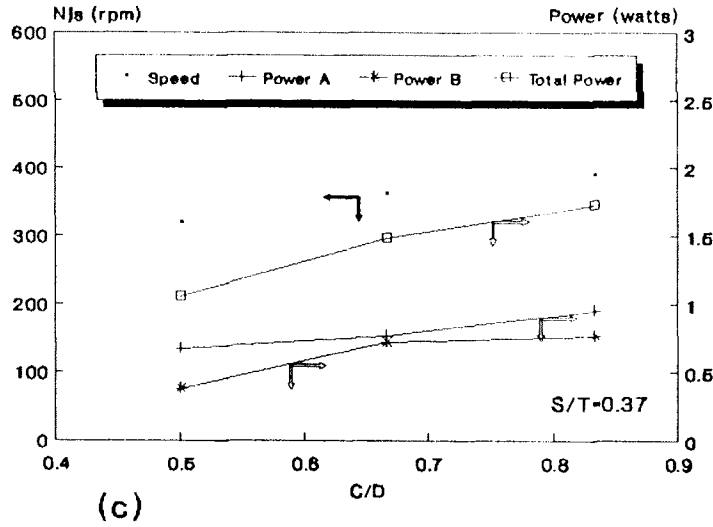


Figure 10. Effect of C on Njs and P

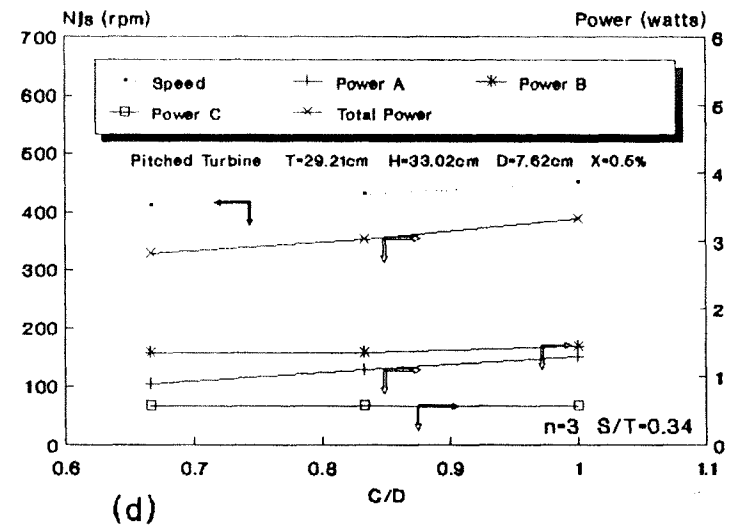
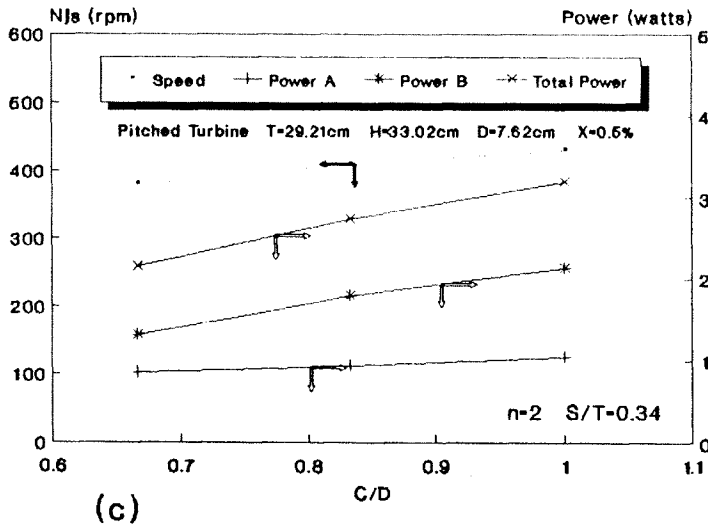
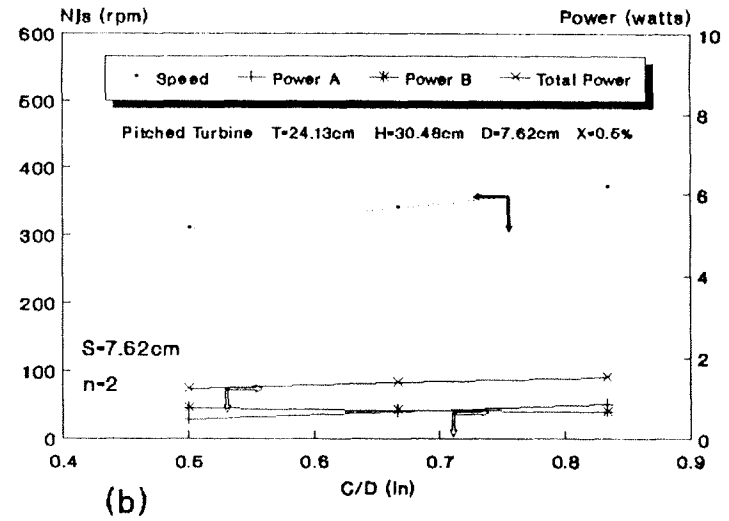
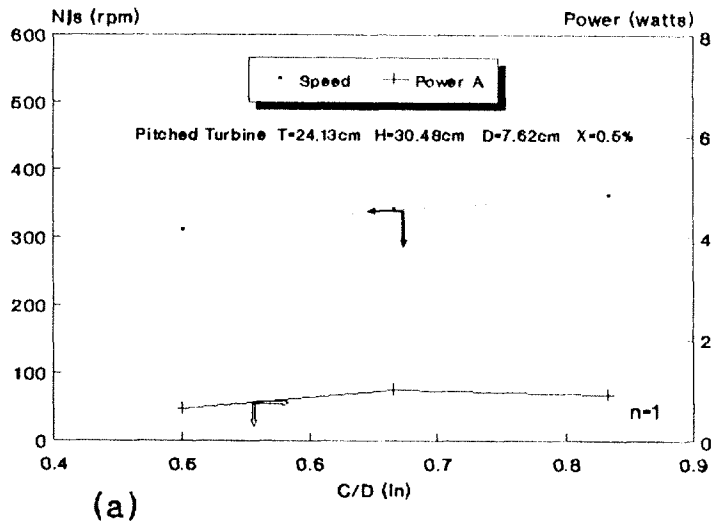
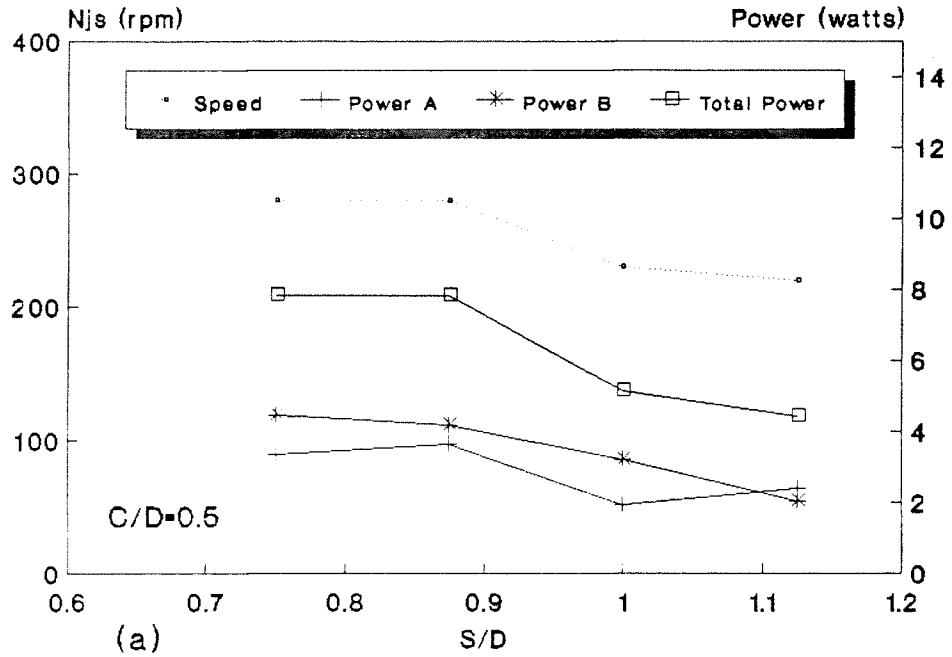


Figure 11. Effect of S on Njs and P



Disc Turbine T=29.21cm H=33.02cm
D=10.16cm n=2

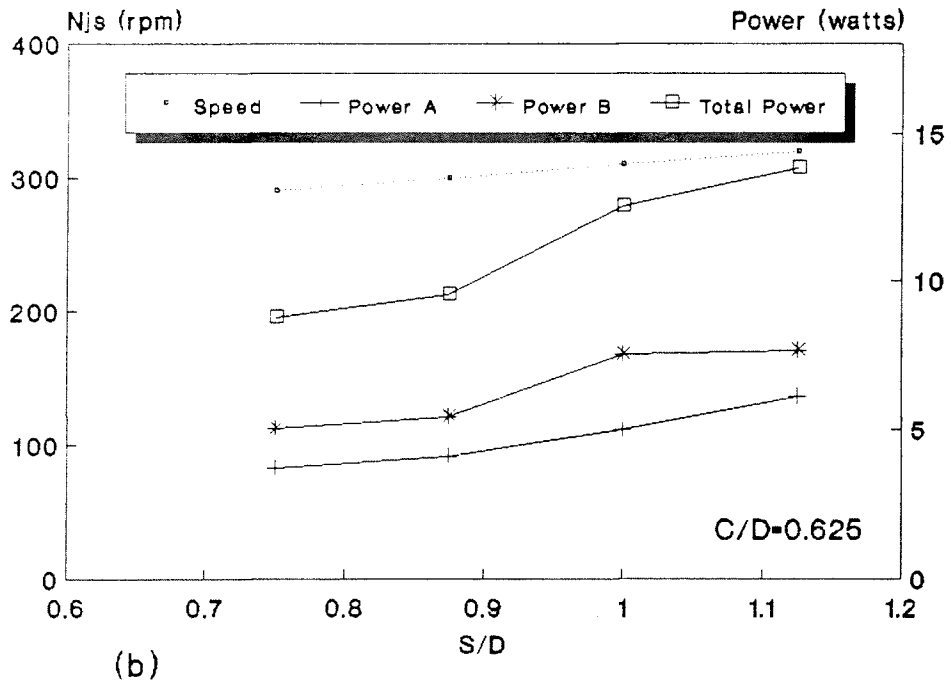
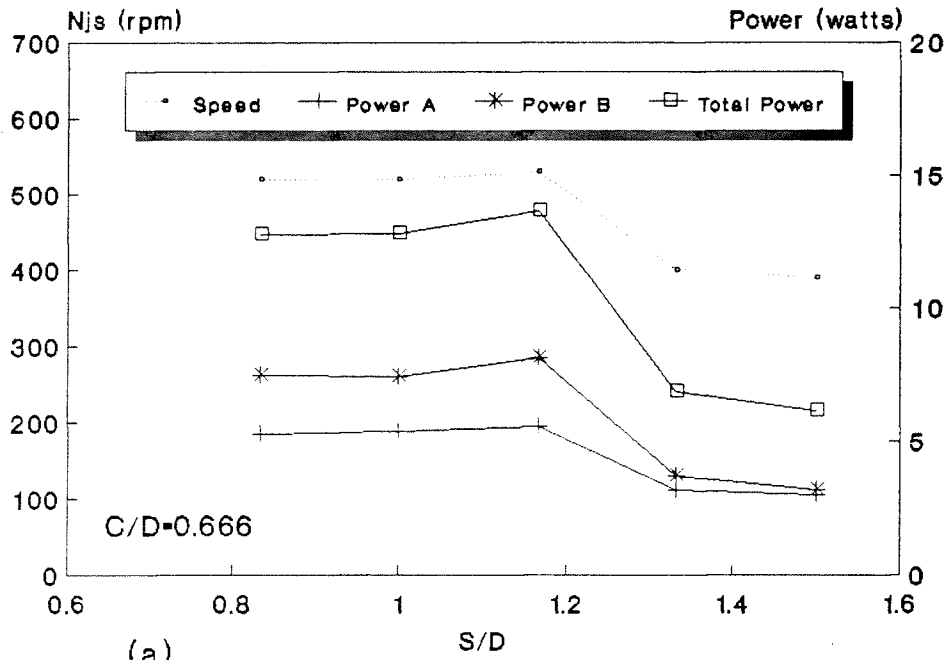
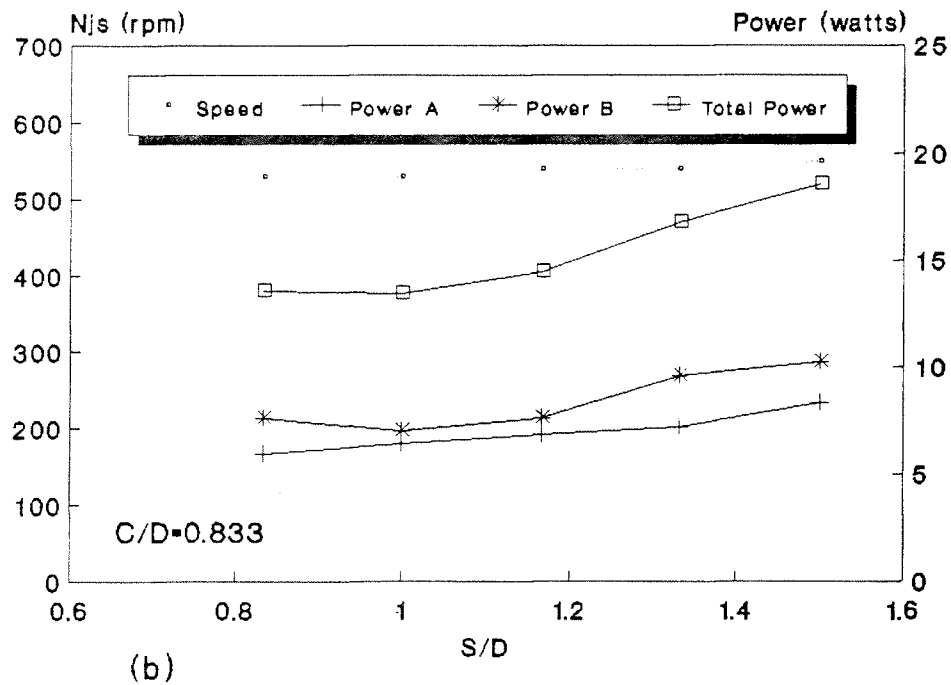


Figure 12. Effect of S on Njs and P

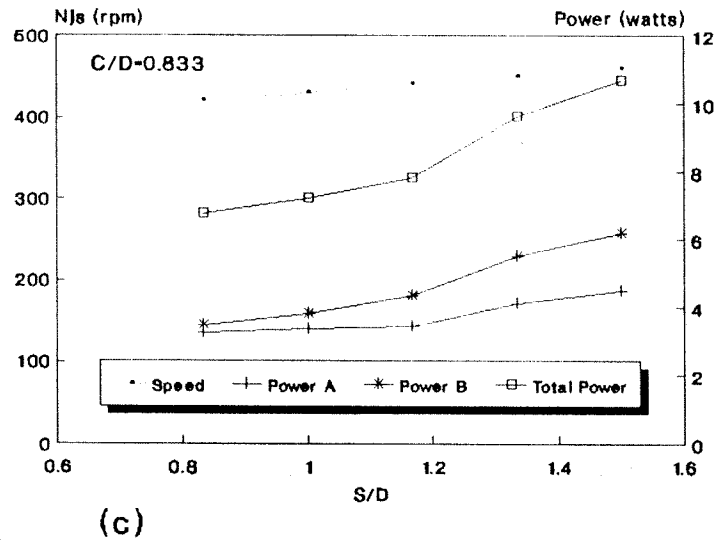
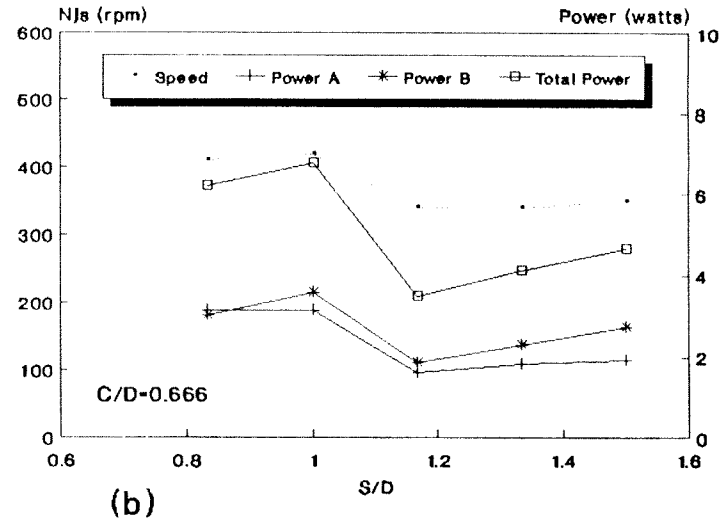
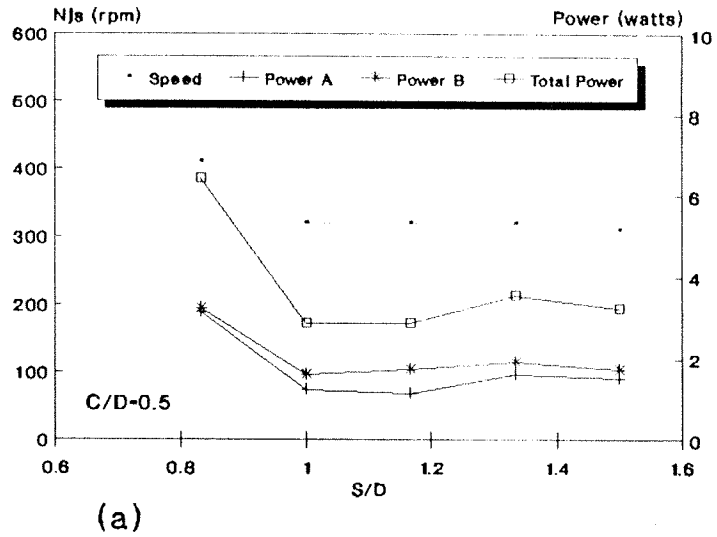


(a)

Disc Turbine T=29.21cm H=33.02cm
D=7.62cm n=2



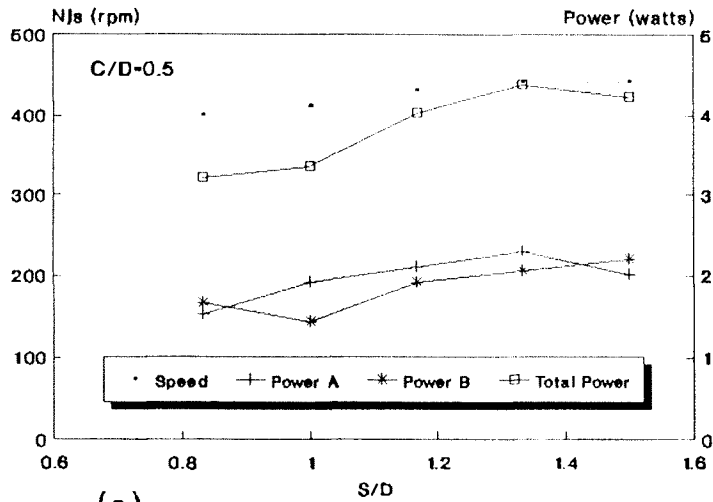
(b)



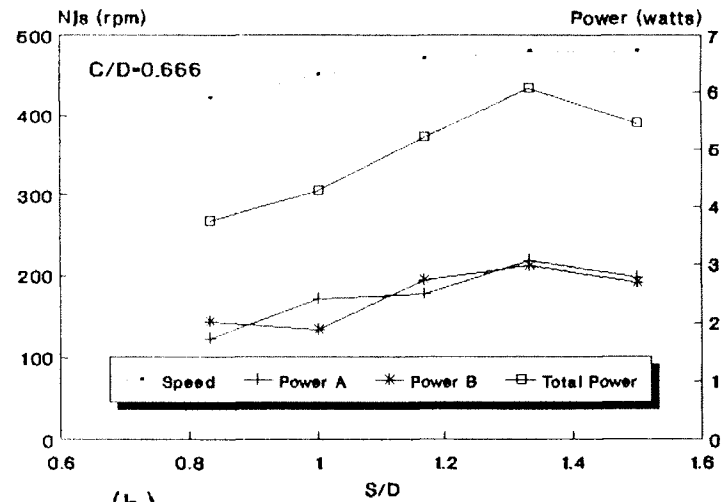
Disc Turbine

T=24.13cm H=30.48cm
 D=7.62cm n=2

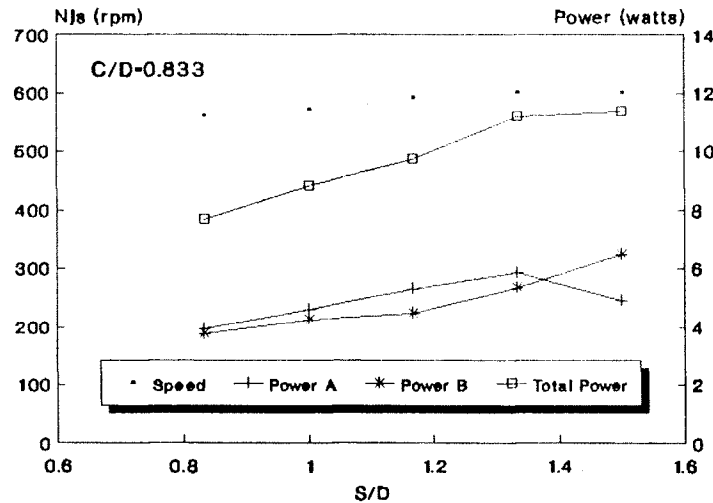
Figure 13. Effect of S on Njs and P



(a)



(b)



(c)

Flat Turbine

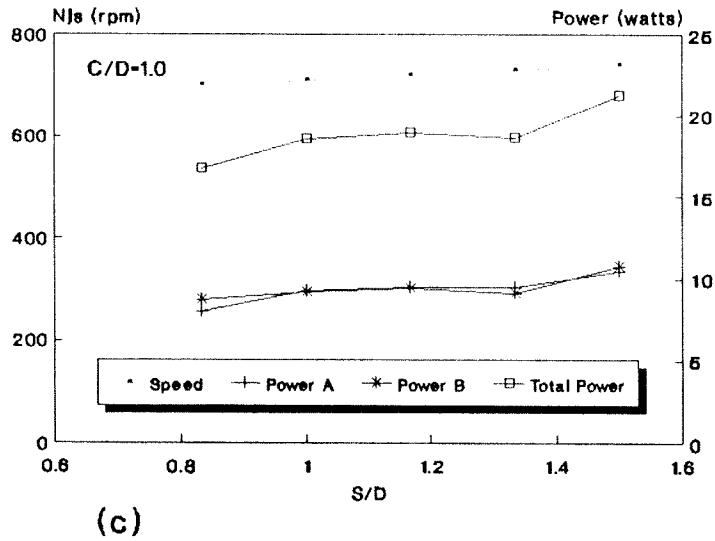
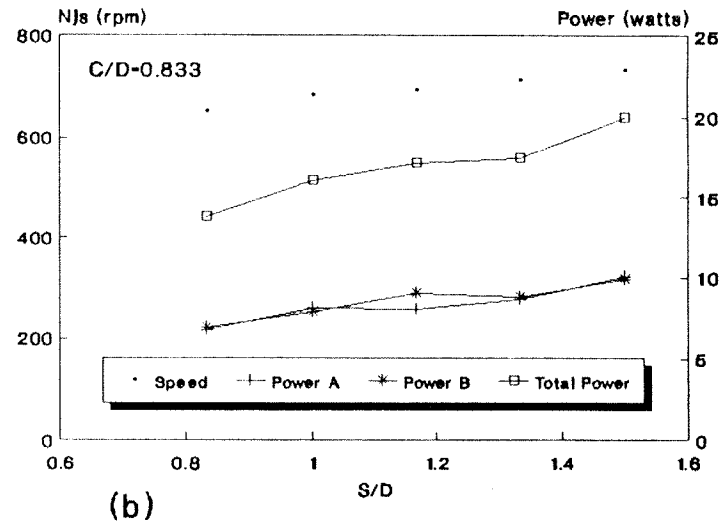
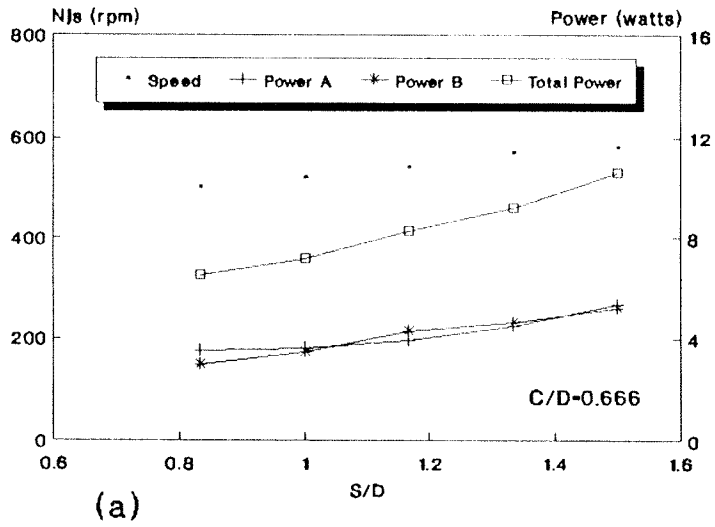
T=24.13cm

H=30.48cm

D=7.62cm

n=2

Figure 14. Effect of S on Njs and P

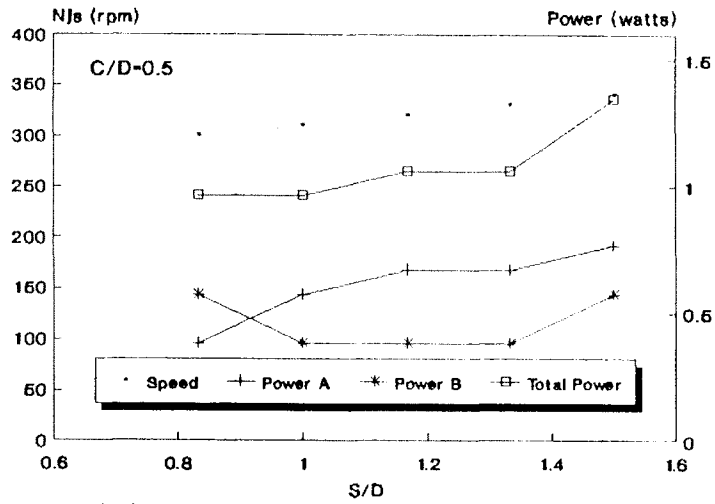


Flat Turbine

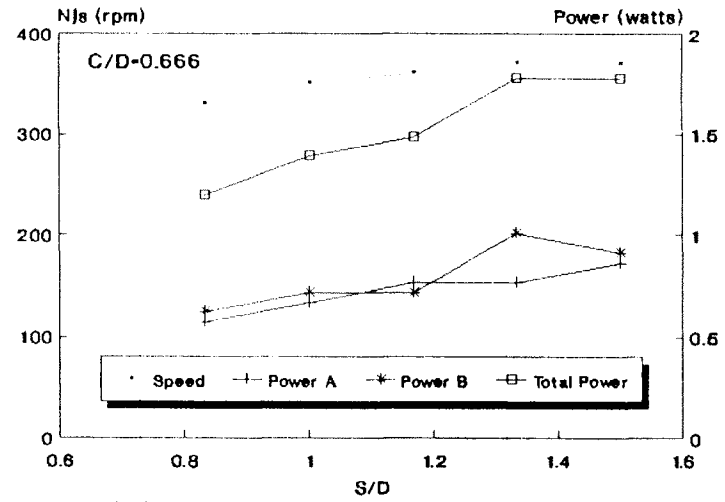
T=29.21cm H=33.02cm

D=7.62cm n=2

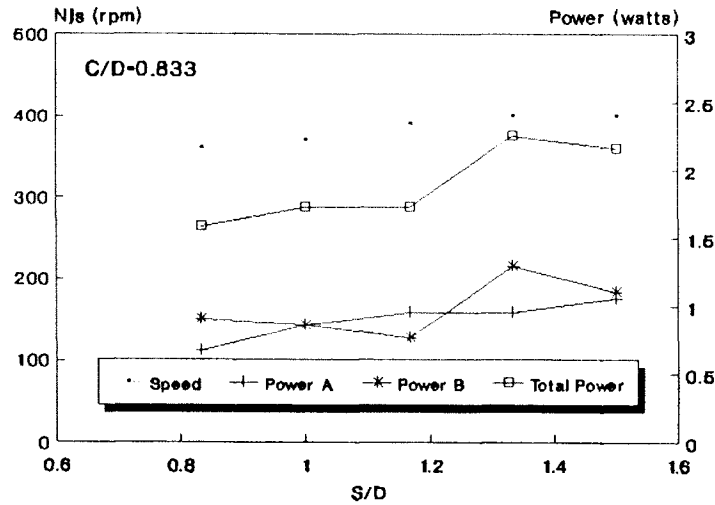
Figure 15. Effect of S on Njs and P



(a)



(b)



(c)

Pitched Turbine

T=24.13cm

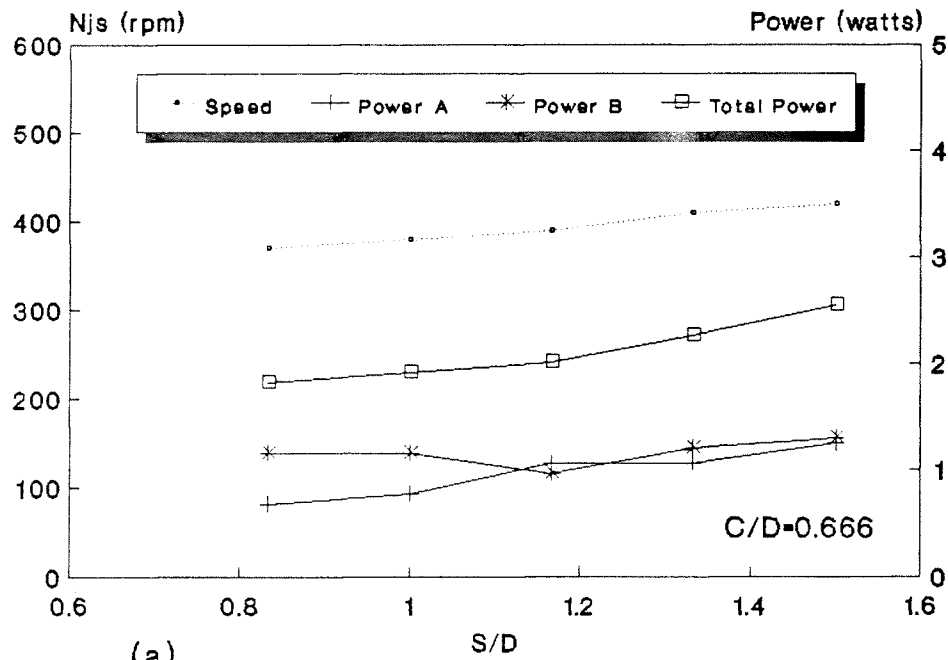
H=30.48cm

D=7.62cm

n=2

Figure 16. Effect of S on Njs and P

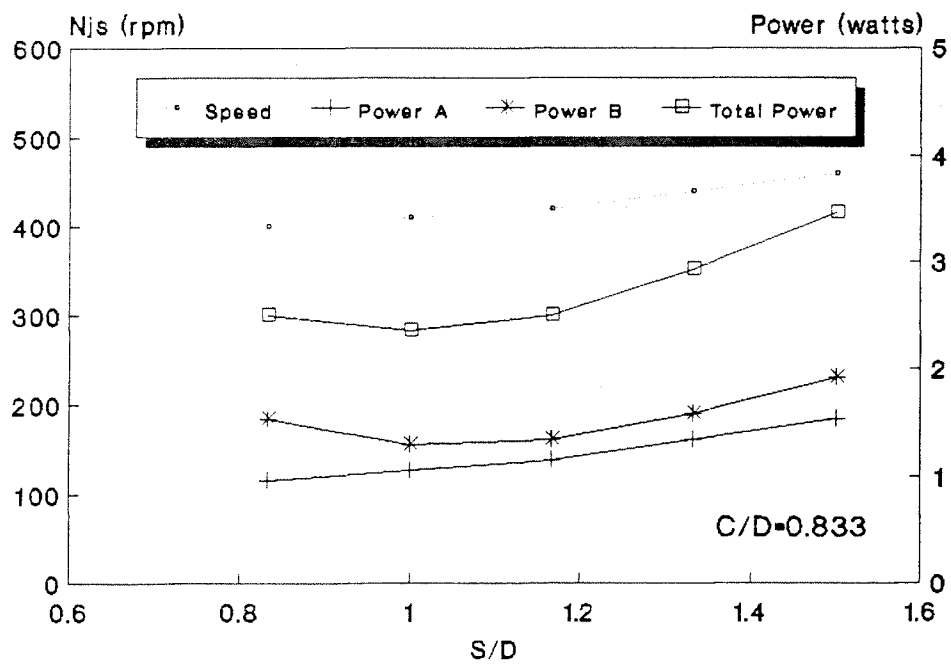
Figure 17. Effect of S on Njs and P



(a)

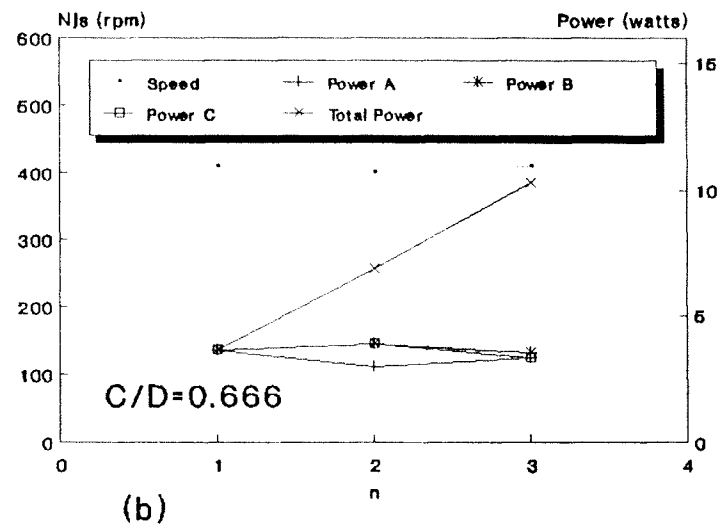
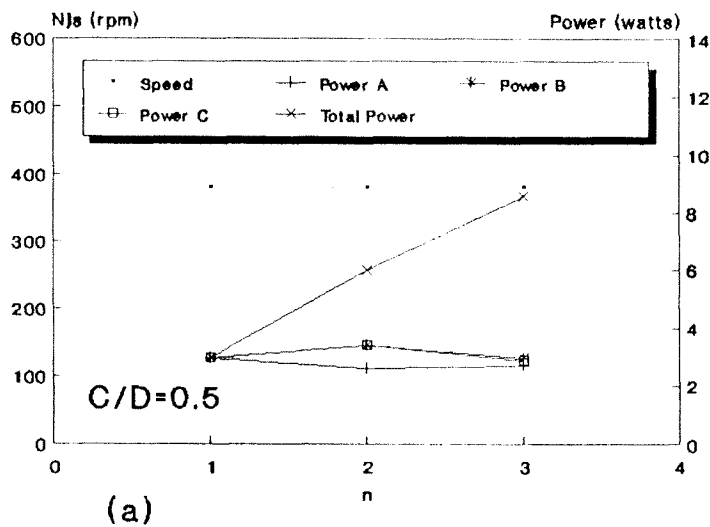
Pitched Turbine

T=29.21cm H=33.02cm D=7.62cm n=2



(b)

Figure 18. Effect of n on Njs and P



Disc Turbine
D=7.62cm

T=29.21cm
S/D=1.333

H=33.02cm

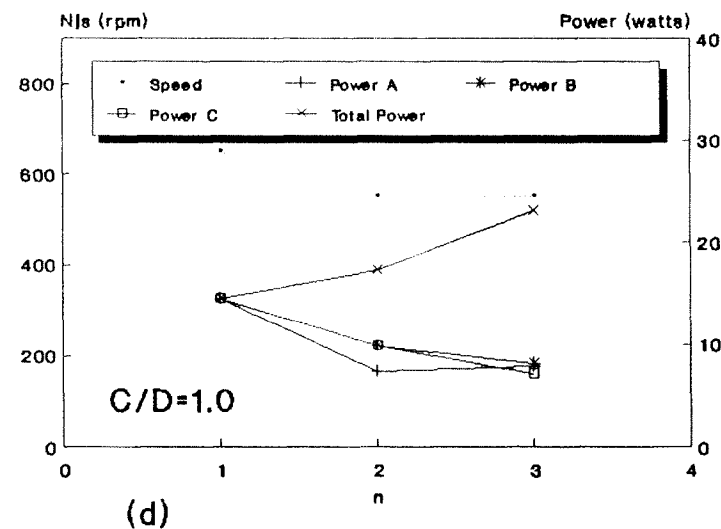
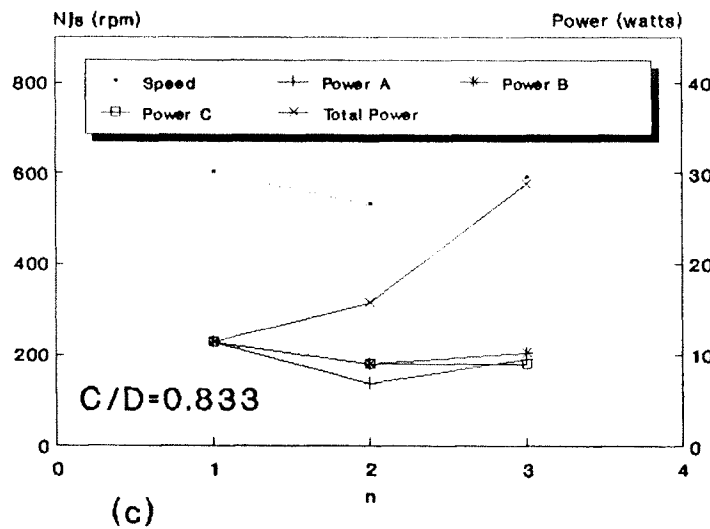
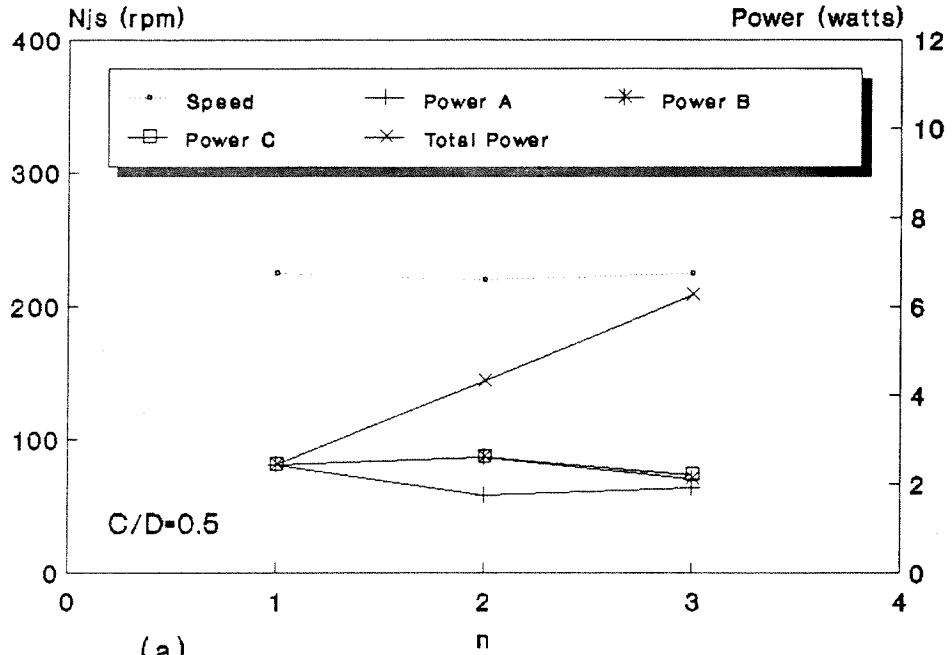
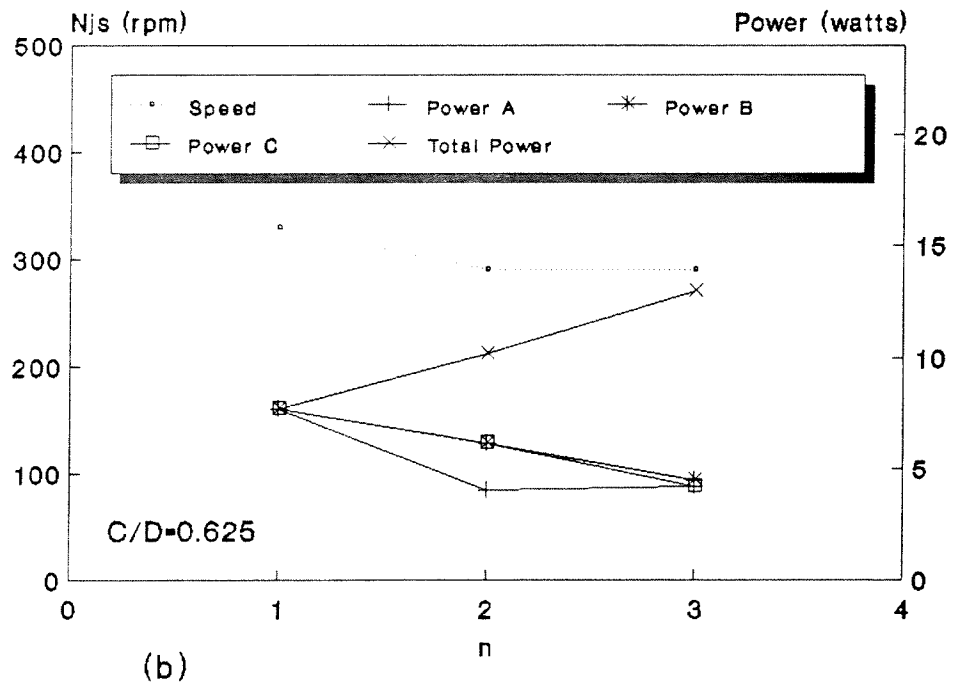
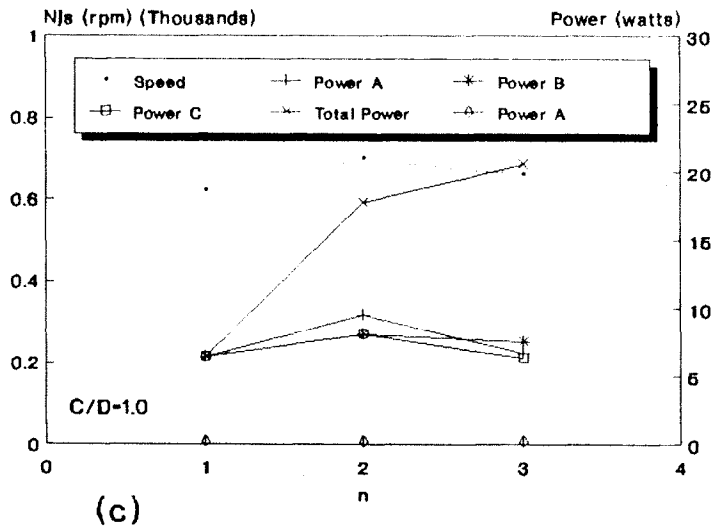
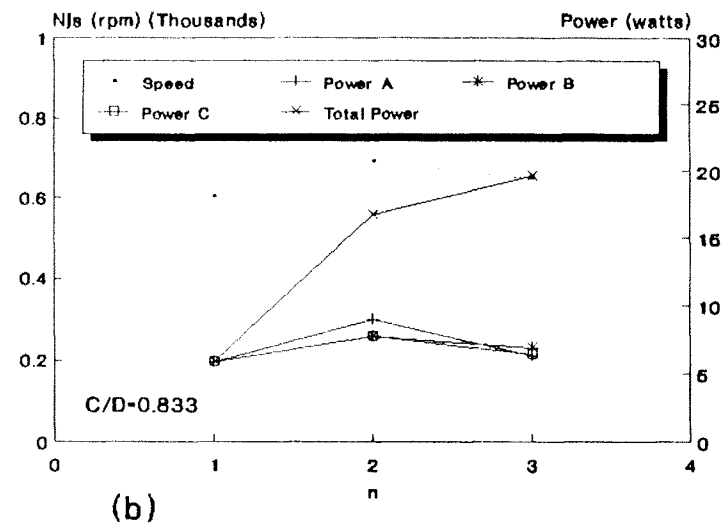
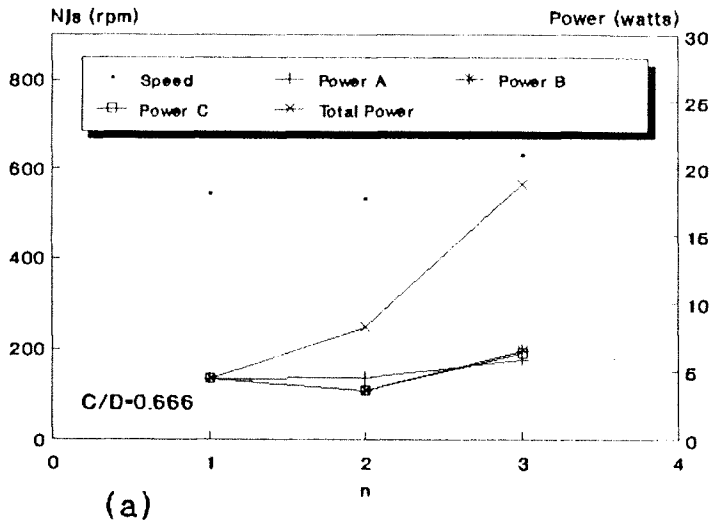


Figure 19. Effect of n on N_{js} and P



Disc Turbine $T=29.21\text{cm}$ $H=33.02\text{cm}$
 $D=10.16\text{cm}$ $S/D=1.0$

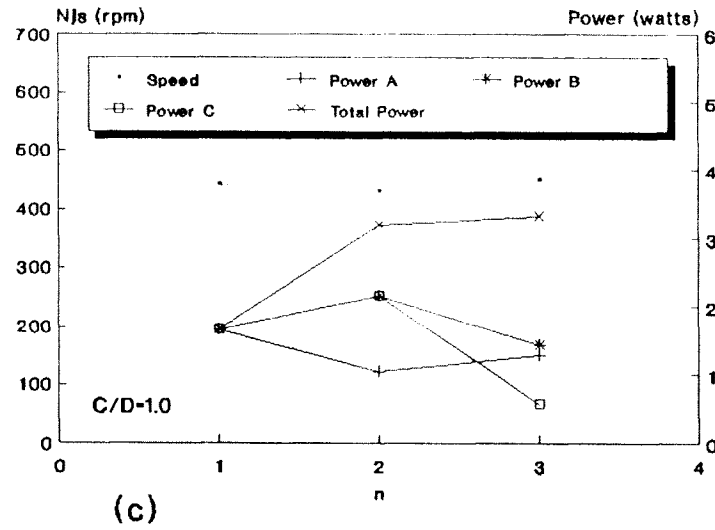
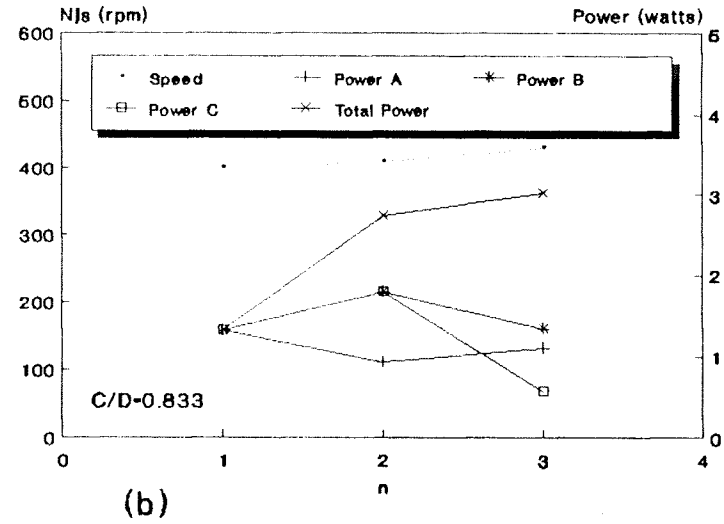
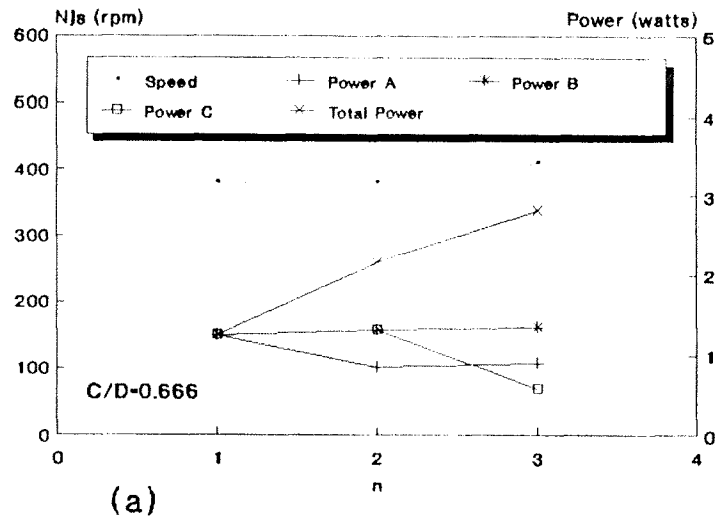




Flat Turbine

T=29.21cm H=33.02cm
 D=7.62cm S/D=1.167

Figure 20. Effect of n on Njs and P



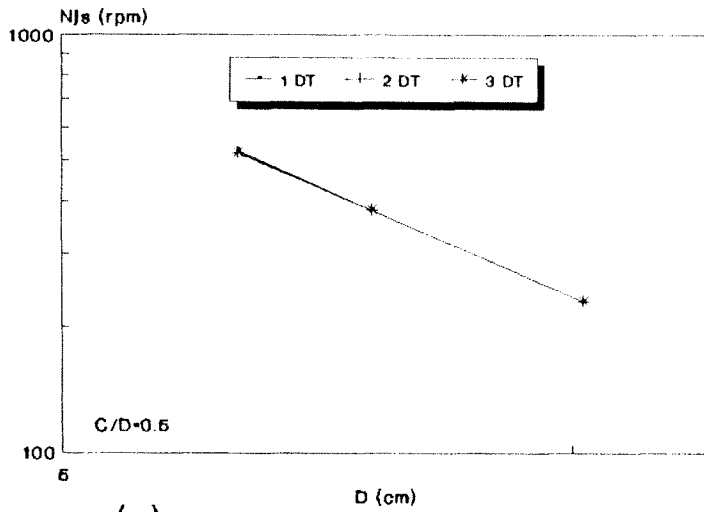
Pitched Turbine

$T=29.21\text{cm}$ $H=33.02\text{cm}$

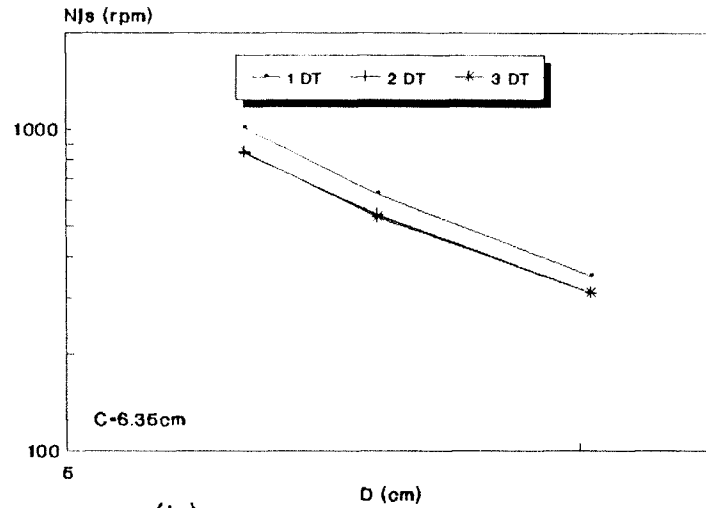
$D=7.62\text{cm}$ $S/D=1.167$

Figure 21. Effect of n on N_{js} and P

Figure 22. Effect of D on Njs

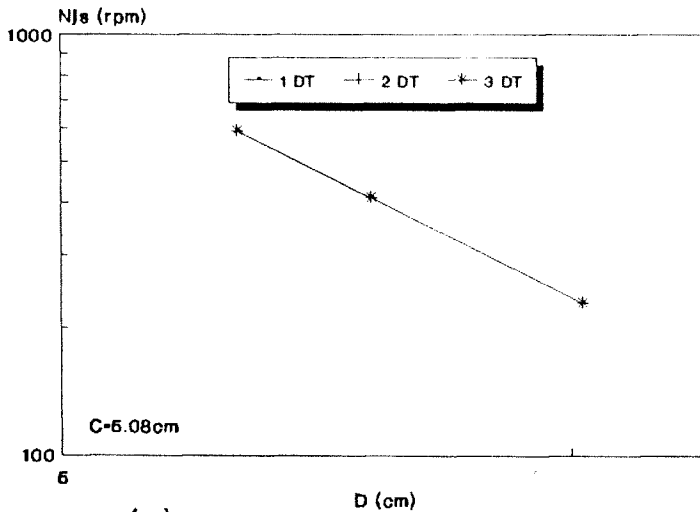


(a)

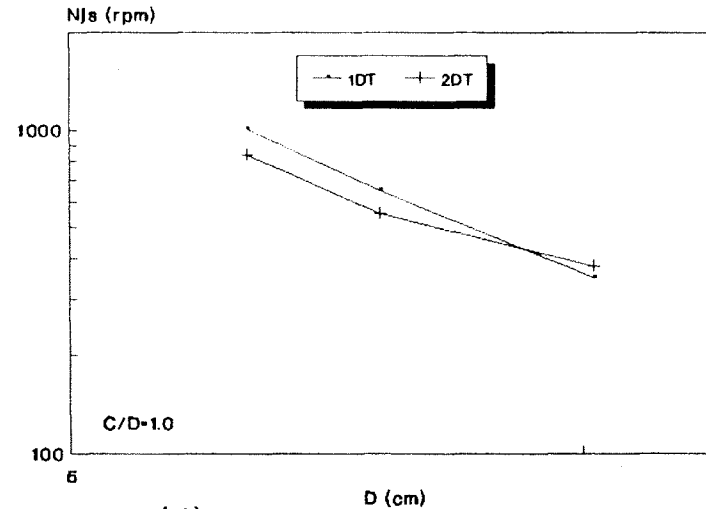


(b)

Disc Turbine T=29.21cm H=33.02cm S=10.16cm

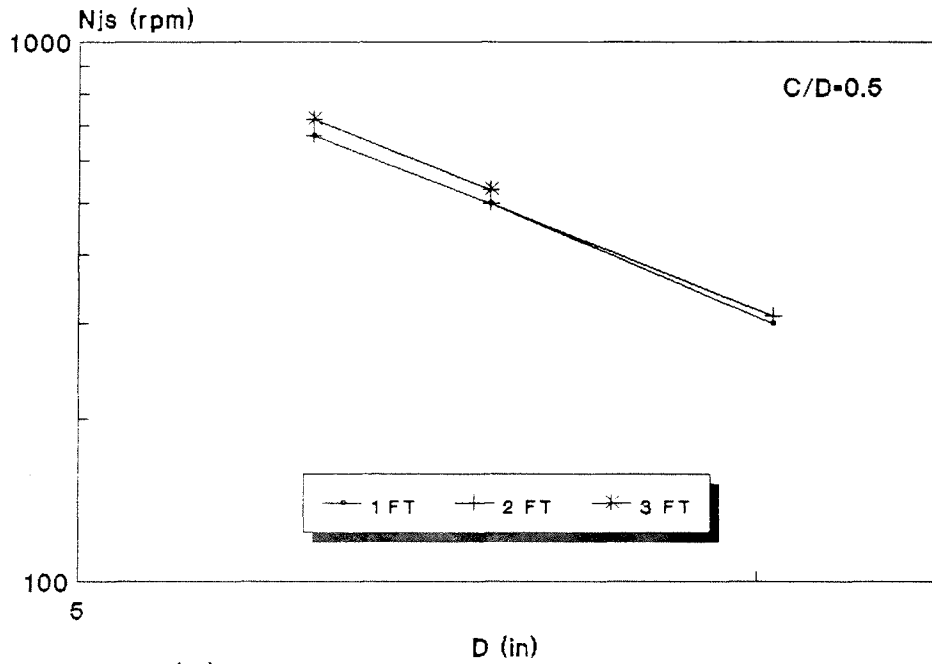


(c)



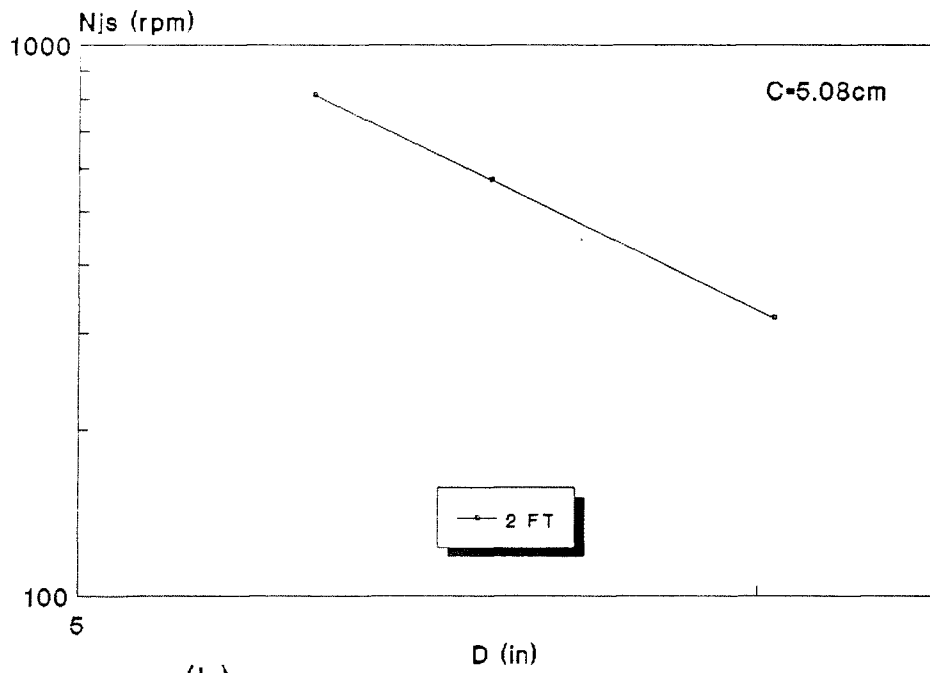
(d)

Figure 23. Effect of D on Njs



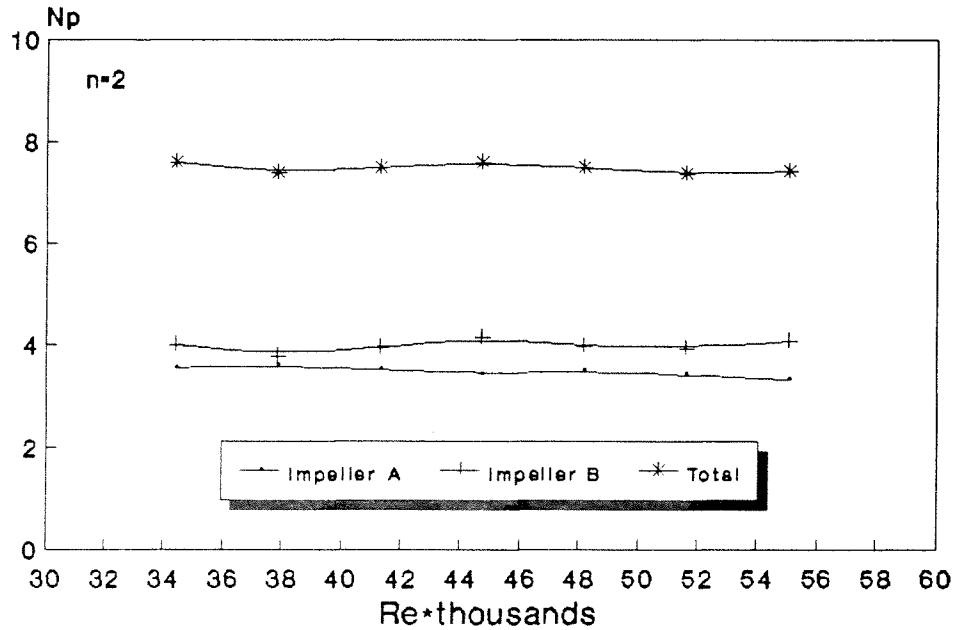
(a)

Flat Turbine T=29.21cm
 H=33.02cm S=10.16cm



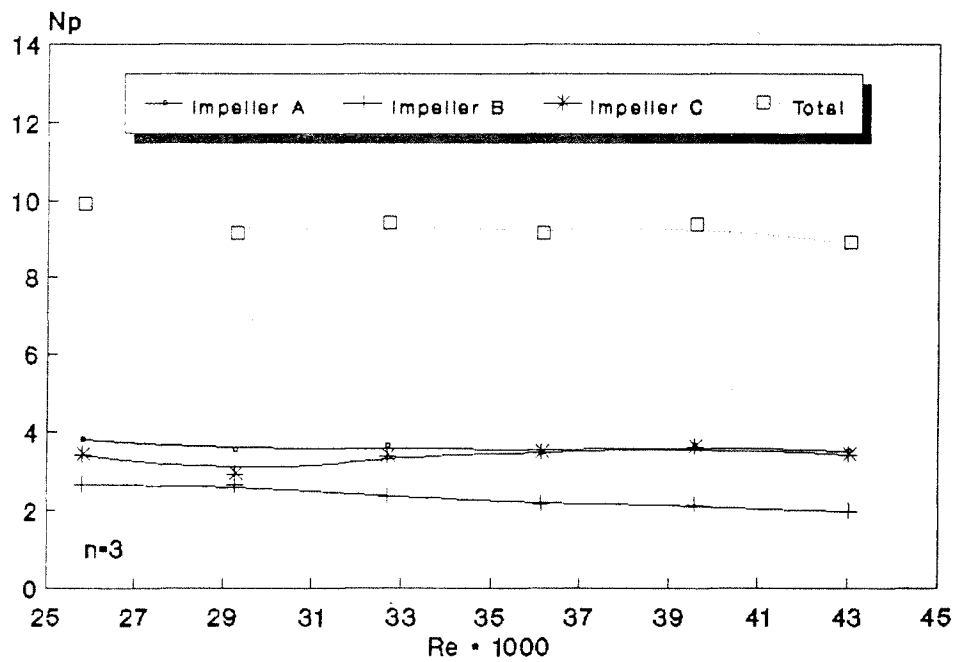
(b)

Figure 24. N_p vs. Re for Multiple Impeller System



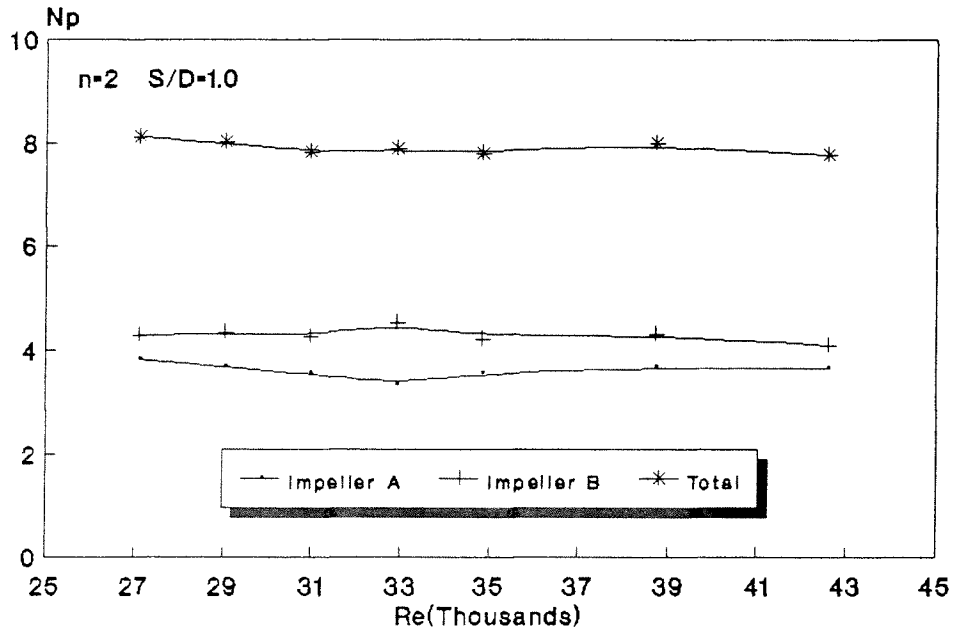
(a)

Disc Turbine $T=29.21\text{cm}$ $D=10.16\text{cm}$
 $H/T=1.39$ $C/D=1.0$ $S/D=1.0$



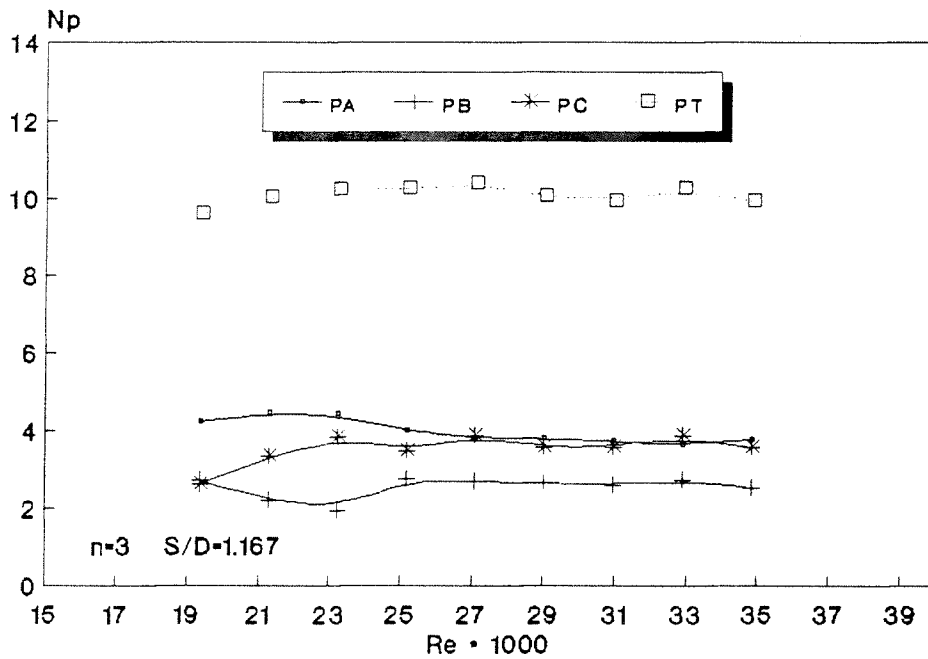
(b)

Figure 25. N_p vs Re for Multiple Impeller System



(a)

Disc Turbine $T=29.21\text{cm}$ $D=7.62\text{cm}$
 $H/T=1.39$ $C/D=1.0$



(b)

Figure 26. Effect of Spacing between Impellers on Power Consumption

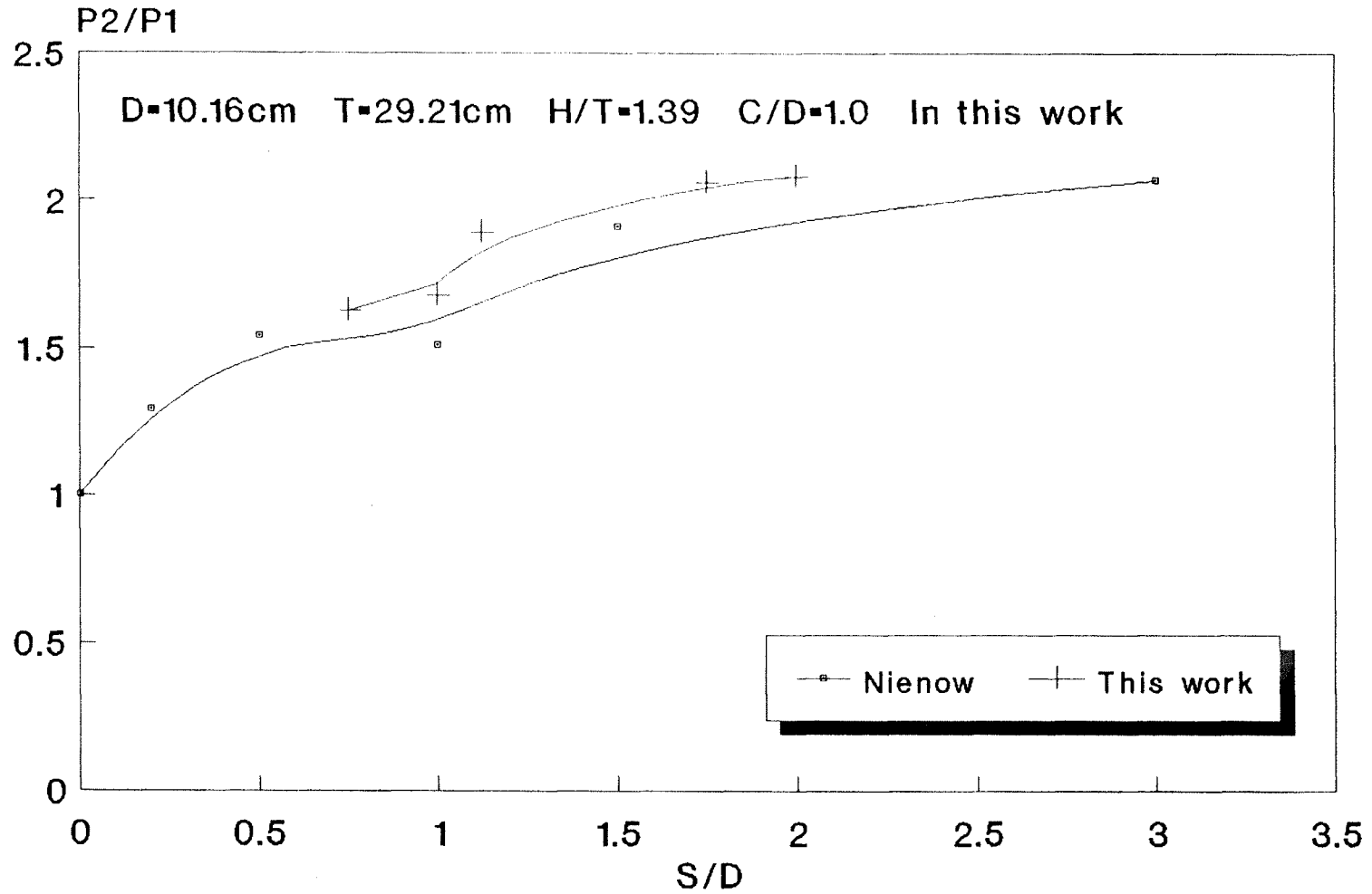
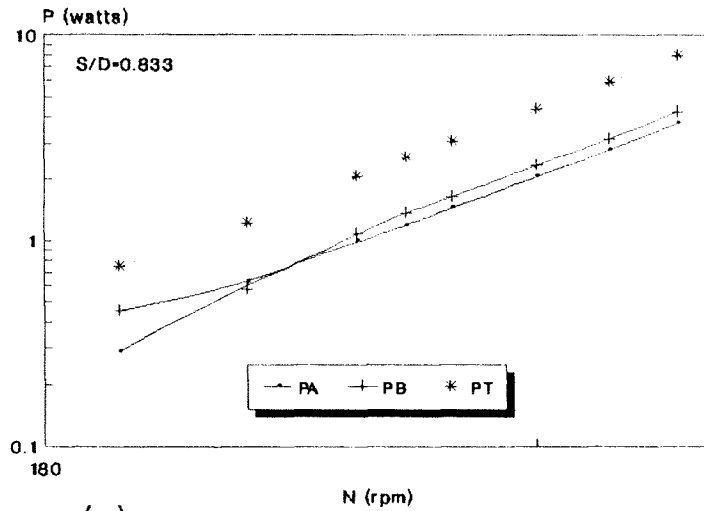
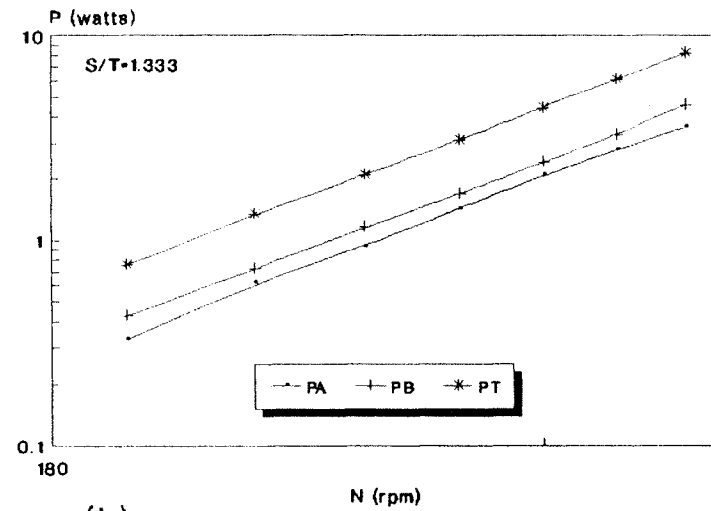


Figure 27. N_p vs. N for Dual Impeller System

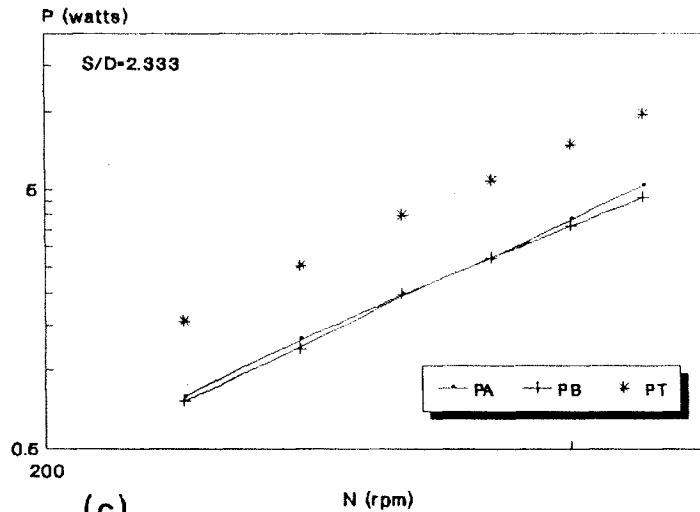


(a)

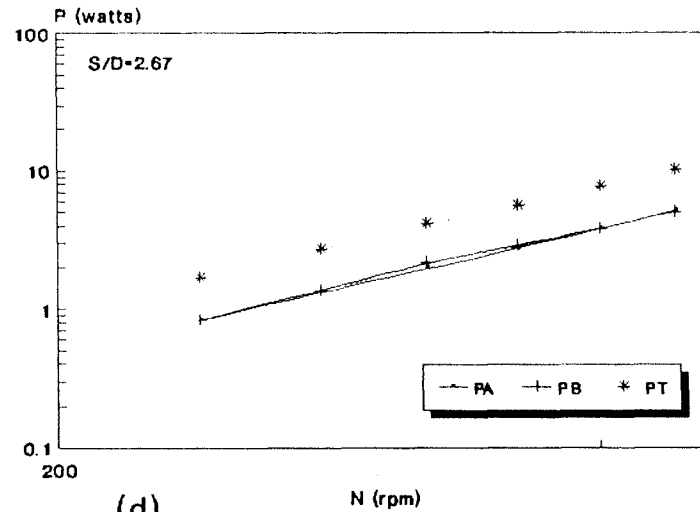


(b)

Disc Turbine $T=29.21\text{cm}$ $D=7.62\text{cm}$ $H/T=1.39$ $C/D=1.0$

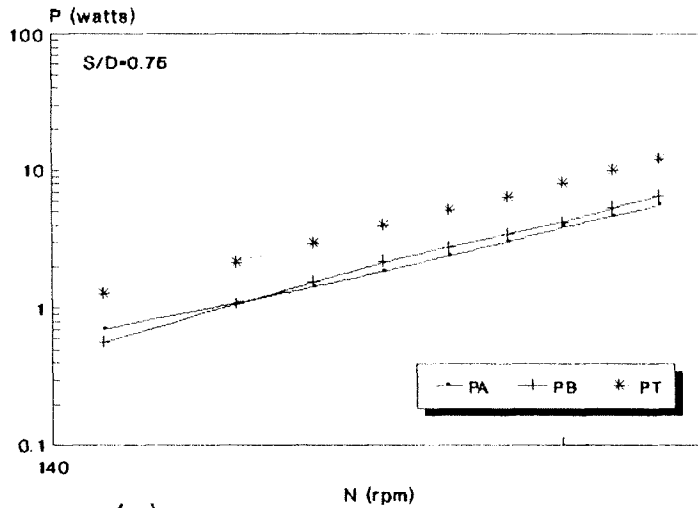


(c)

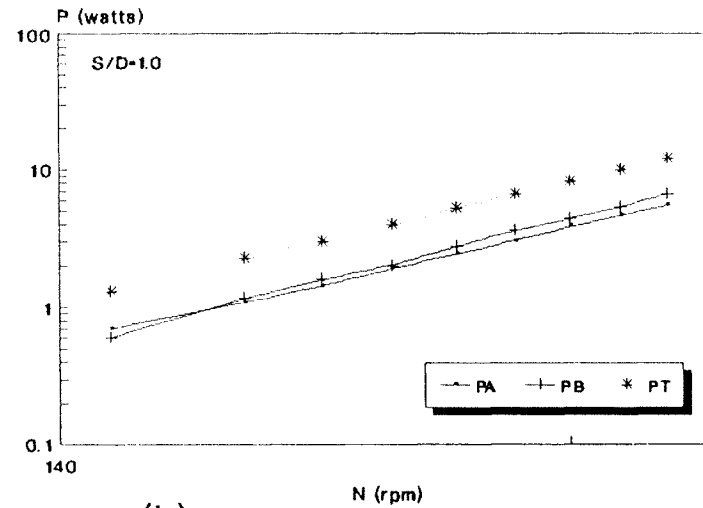


(d)

Figure 28. P vs N for The Two Impeller System

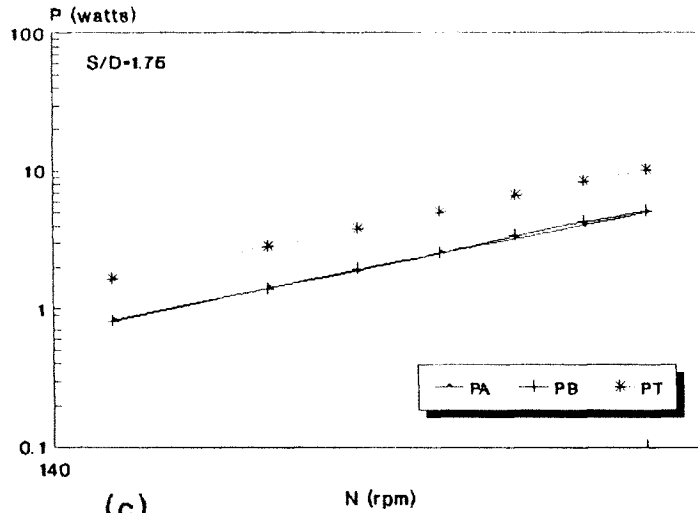


(a)

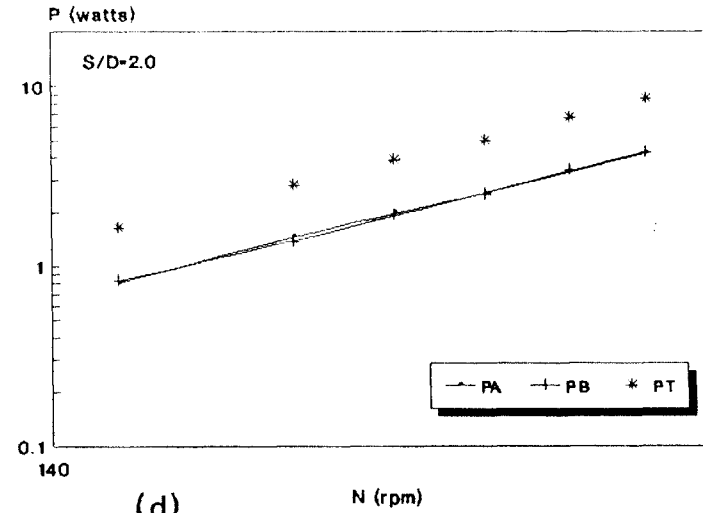


(b)

Disc Turbine $T=29.21\text{cm}$ $D=10.16\text{cm}$ $H/T=1.39$ $C/D=1.0$



(c)



(d)

Appendices

Experimental Data

Effect of Spacing between Impellers on Minimum Suspension Speed

Disc Turbine, $n=2$, $D=10.16\text{cm}$, $T=29.21\text{cm}$, $H=33.02\text{cm}$, $dp=110\mu\text{m}$, $x=0.5\%$ (weight)

S (cm)	C/D	N_{js} (rpm)	PA (watts)	PB (watts)	PC (watts)	PT (watts)
7.62	0.5	280	3.36	4.47		7.83
8.89		280	3.65	4.18		7.83
10.16		230	1.92	3.22		5.14
11.43		220	2.40	2.02		4.42
7.62	0.625	290	3.75	5.04		8.79
8.89		300	4.13	5.43		9.56
10.16		310	4.99	7.54		12.53
11.43		320	6.15	7.68		13.83

**Effect of Spacing between Impellers
on Minimum Suspension Speed**

Disc Turbine, $D=7.62\text{cm}$, $n=2$, $T=29.21\text{ cm}$, $H=33.02\text{ cm}$, $dp=110\ \mu\text{m}$, $x=0.5\%$ (weight)

S (cm)	C/D	N_{js} (rpm)	PA (watts)	PB (watts)	PC (watts)	PT (watts)
6.35	0.666	520	5.28	7.49		12.77
7.62		520	5.37	7.44		12.82
8.89		530	5.57	8.12		13.69
10.16		400	3.17	3.70		6.87
11.43		390	2.98	3.17		6.15
6.35	0.833	530	5.95	7.64		13.59
7.62		530	6.44	7.01		13.45
8.89		540	6.82	7.64		14.46
10.16		540	7.20	9.56		16.76
11.43		550	8.36	10.23		18.59

**Effect of Spacing between Impellers
on Minimum Suspension Speed**

Pitched Turbine, D=7.62cm, n=2, T=29.21cm, H=33.02cm, dp=110 μ m, x=0.5%(weight)

S (cm)	C/D	N _{js} (rpm)	PA (watts)	PB (watts)	PC (watts)	PT (watts)
6.35	0.666	370	0.67	1.15		1.82
7.62		380	0.77	1.15		1.92
8.89		390	1.06	0.96		2.02
10.16		410	1.06	1.20		2.26
11.43		420	1.25	1.29		2.54
6.35	0.833	400	0.96	1.54		2.50
7.62		410	1.06	1.30		2.36
8.89		420	1.15	1.34		2.49
10.16		440	1.34	1.58		2.92
11.43		460	1.54	1.92		3.46

**Effect of Spacing between Impellers
on Minimum Suspension Speed**

Flat Turbine, D=7.62cm, n=2, T=29.21 cm, H=33.02 cm, dp=110 μ m, x=0.5%(weight)

S (cm)	C/D	N _{js} (rpm)	PA (watts)	PB (watts)	PC (watts)	PT (watts)
6.35	0.666	500	3.55	2.98		6.53
7.62		520	3.65	3.51		7.16
8.89		540	3.94	4.32		8.26
10.16		570	4.51	4.66		9.17
11.43		580	5.38	5.19		10.57
6.35	0.833	650	6.82	6.96		13.78
7.62		680	8.16	7.88		16.04
8.89		690	8.07	9.08		17.15
10.16		710	8.64	8.84		17.48
11.43		730	10.09	9.94		20.03
6.35	1.0	700	8.07	8.74		16.81
7.62		710	9.32	9.26		18.58
8.89		720	9.51	9.46		18.97
10.16		730	9.51	9.12		18.63
11.43		740	10.47	10.81		21.28

**Effect of Spacing between Impellers
on Minimum Suspension Speed**

Disc Turbine, $D=7.62\text{cm}$, $n=2$, $T=24.13\text{cm}$, $H=30.48\text{cm}$, $dp=110\ \mu\text{m}$, $x=0.5\%$ (weight)

S (cm)	C/D	N_{js} (rpm)	PA (watts)	PB (watts)	PC (watts)	PT (watts)
6.35	0.5	410	3.17	3.27		6.44
7.62		320	1.25	1.63		2.88
8.89		320	1.15	1.73		2.88
10.16		320	1.63	1.92		3.55
11.43		310	1.54	1.73		3.27
6.35	0.666	410	3.17	3.03		6.20
7.62		420	3.17	3.60		6.77
8.89		340	1.63	1.87		3.50
10.16		340	1.83	2.30		4.13
11.43		350	1.92	2.74		4.66
6.35	0.833	420	3.26	3.51		6.77
7.62		430	3.36	3.84		7.20
8.89		440	3.46	4.37		7.83
10.16		450	4.13	5.52		9.65
11.43		460	4.51	6.19		10.70

**Effect of Spacing between Impellers
on Minimum Suspension Speed**

Flat Turbine, D=7.62cm, n=2, T=24.13cm, H=30.48cm, dp=110 μm, x=0.5%(weight)

S (cm)	C/D	N _{js} (rpm)	PA (watts)	PB (watts)	PC (watts)	PT (watts)
6.35	0.5	400	1.54	1.68		3.22
7.62		410	1.92	1.44		3.36
8.89		430	2.11	1.92		4.03
10.16		440	2.30	2.07		4.37
11.43		440	2.02	2.21		4.23
6.35	0.666	420	1.73	2.02		3.75
7.62		450	2.40	1.87		4.27
8.89		470	2.50	2.74		5.24
10.16		480	3.07	2.98		6.05
11.43		480	2.79	2.69		5.48
6.35	0.833	560	3.94	3.74		7.68
7.62		570	4.61	4.23		8.84
8.89		590	5.28	4.47		9.75
10.16		600	5.86	5.33		11.19
11.43		600	4.90	6.48		11.38

**Effect of Spacing between Impellers
on Minimum Suspension Speed**

Pitched Turbine, D=7.62cm, n=2, T=24.13cm, H=30.48cm, dp=110 μ m, x=0.5%(weight)

S (cm)	C/D	N _{js} (rpm)	PA (watts)	PB (watts)	PC (watts)	PT (watts)
6.35	0.5	300	0.38	0.58		0.96
7.62		310	0.58	0.38		0.96
8.89		320	0.67	0.38		1.05
10.16		330	0.67	0.38		1.05
11.43		340	0.77	0.57		1.34
6.35	0.666	330	0.58	0.62		1.20
7.62		350	0.67	0.72		1.39
8.89		360	0.77	0.72		1.49
10.16		370	0.77	1.01		1.78
11.43		370	0.86	0.91		1.77
6.35	0.833	360	0.67	0.91		1.58
7.62		370	0.86	0.86		1.72
8.89		390	0.96	0.77		1.73
10.16		400	0.96	1.30		2.26
11.43		400	1.06	1.10		2.16

**Effect of Number of Impellers on
Minimum Suspension Speed and Power**

Disc Turbine, D=10.16cm, T=29.21 cm, H=33.02 cm, dp=110 μ m, x=0.5%(weight)

n	S (cm)	C/D	N _{js} (rpm)	PA (watt)	PB (watt)	PC (watt)	PT (watt)
1	10.16	0.5	225	2.43			2.43
2			220	1.73	2.59		4.32
3			225	1.92	2.11	2.21	6.24
1	10.16	0.625	330	7.72			7.72
2			290	4.03	6.15		10.18
3			290	4.23	4.51	4.23	12.97

**Effect of Number of Impellers on
Minimum Suspension Speed and Power**

Disc Turbine, D=7.62cm, T=29.21cm, H=33.02cm, dp=110 μm, x=0.5%(weight)

n	S (cm)	C/D	N _{js} (rpm)	PA (watt)	PB (watt)	PC (watt)	PT (watt)
1	10.16	0.5	380	2.95			2.95
2			380	2.59	3.41		6.0
3			380	2.69	2.98	2.88	8.55
1	10.16	0.666	410	3.62			3.62
2			400	2.98	3.89		6.87
3			410	3.36	3.55	3.36	10.28
1	10.16	0.833	600	11.33			11.33
2			530	6.82	8.98		15.80
3			590	9.51	10.18	9.03	28.72
1	10.16	1.0	650	14.54			14.54
2			550	7.40	9.89		17.29
3			550	7.88	8.07	7.11	23.06

**Effect of Number of Impellers
on Minimum Suspension Speed**

Disc Turbine, D=2.5 in, T=29.21cm, H=33.02cm, dp=110 μ m, x=0.5%(weight)

n	S (cm)	C/D	N _{js} (rpm)
1	10.16	0.5	530
2			520
3			520
1	10.16	0.7	560
2			550
3			570
1	10.16	0.8	590
2			590
3			590
1	10.16	1.0	1010
2			840
3			850

**Effect of Number of Impellers
on Minimum Suspension Speed**

Pitched Turbine, D=7.62cm, T=29.21cm, H=33.02cm, dp=110 μm, x=0.5%(weight)

n	S (cm)	C/D	N _{js} (rpm)	PA (watt)	PB (watt)	PC (watt)	PT (watt)
1	8.89	0.666	380	1.25			1.25
2			380	0.85	1.31		2.16
3			410	0.90	1.34	0.58	2.82
1	8.89	0.833	400	1.33			1.33
2			410	0.94	1.80		2.74
3			430	1.1	1.34	0.58	3.02
1	8.89	1.0	440	1.67			1.67
2			430	1.05	2.15		3.20
3			450	1.30	1.44	0.58	3.32

**Effect of Number of Impellers
on Minimum Suspension Speed**

Flat Turbine, D=7.62cm, T=29.21cm, H=33.02cm, dp=110 μm, x=0.5%(weight)

n	S (cm)	C/D	N _{js} (rpm)	PA (watt)	PB (watt)	PC (watt)	PT (watt)
1	8.89	0.666	540	4.45			4.45
2			530	4.60	3.66		8.26
3			630	5.90	6.53	6.34	18.77
1	8.89	0.833	600	5.89			5.89
2			690	9.40	7.36		16.76
3			650	6.60	6.92	6.44	19.95
1	8.89	1.0	620	6.50			6.50
2			700	9.60	8.12		17.72
3			660	6.70	7.59	6.34	20.63

**Effect of Number of Impellers on
Minimum Suspension Speed and Power**

Disc Turbine, D=7.62cm, T=24.13cm, H=30.48cm, dp=110 μ m, x=0.5% (weight)

n	S (cm)	C/D	N _{js} (rpm)	PA (watt)	PB (watt)	PC (watt)	PT (watt)
1	7.62	0.5	320	1.92			1.92
2			320	1.25	1.78		3.03
3			310				
1	7.62	0.666	490	6.79			6.79
2			410	2.59	3.84		6.43
3			450				
1	7.62	0.833	510	7.62			7.62
2			440	3.07	4.56		7.63
3			520				

**Effect of Number of Impellers on
Minimum Suspension Speed and Power**

Flat turbine, D=7.62cm, T=24.13cm, H=30.48cm, dp=110 μ m, x=0.5%(weight)

n	S (cm)	C/D	N _s (rpm)	PA (watt)	PB (watt)	PC (watt)	PT (watt)
1	7.62	0.5	410	1.86			1.86
2			410	1.54	1.68		3.22
3			500				
1	7.62	0.666	460	2.63			2.63
2			450	1.92	2.35		4.27
3			500				
1	7.62	0.833	500	3.39			3.39
2			570	4.13	4.08		8.21
3			560				

**Effect of Number of Impellers on
Minimum Suspension Speed and Power**

Flat turbine, D=7.62cm, T=24.13cm, H=30.48cm, dp=110 μ m, x=0.5%(weight)

n	S (cm)	C/D	N _{js} (rpm)	PA (watt)	PB (watt)	PC (watt)	PT (watt)
1	7.62	0.5	310	0.64			0.64
2			310	0.48	0.77		1.25
3			340				
1	7.62	0.666	340	1.02			1.02
2			340	0.67	0.72		1.39
3			370				
1	7.62	0.833	360	0.93			0.93
2			370	0.86	0.67		1.53
3			410				

Effect of Spacing between Impellers on Power Consumption

Disc turbines, $n=2$, $D=7.62\text{cm}$, $T=29.21\text{cm}$, $H=40.64\text{cm}$, $C/D=1.0$

S (cm)	Speed (rpm)	P_A (watts)	P_B (watts)	P_T (watts)	N_p A	N_p B	N_p Total
6.35	240	0.63	0.58	1.21	3.83	3.53	7.36
	280	0.99	1.08	2.07	3.79	4.14	7.93
	320	1.45	1.64	3.09	3.72	4.21	7.93
	360	2.05	2.33	4.38	3.69	4.20	7.89
	400	2.79	3.16	5.95	3.67	4.15	7.82
	440	3.76	4.24	8.00	3.71	4.18	7.89
7.62	240	0.70	0.66	1.36	4.25	4.01	8.27
	280	1.00	1.12	2.12	3.83	4.29	8.12
	320	1.38	1.66	3.04	3.54	4.26	7.80
	360	1.98	2.35	4.33	3.57	4.23	7.80
	400	2.80	3.29	6.09	3.68	4.32	8.00
	440	3.71	4.16	7.87	3.66	4.11	7.77
10.16	240	0.62	0.73	1.35	3.77	4.44	8.21
	280	0.93	1.16	2.09	3.56	4.44	8.00
	320	1.43	1.68	3.11	3.67	4.31	7.98
	360	2.07	2.40	4.47	3.73	4.32	8.05
	400	2.78	3.32	6.10	3.65	4.36	8.01
	440	3.60	4.58	8.18	3.55	4.52	8.07
17.78	240	0.79	0.76	1.55	4.80	4.62	9.43
	280	1.32	1.21	2.53	5.06	4.63	9.69
	320	1.97	1.97	3.94	5.05	5.05	10.11
	360	2.69	2.72	5.41	4.85	4.90	9.77
	400	3.82	3.61	7.43	5.02	4.74	9.76
	440	5.18	4.62	9.80	5.11	4.56	9.67
20.32	240	0.83	0.84	1.67	5.05	5.11	10.16
	280	1.33	1.36	2.69	5.09	5.21	10.30
	320	1.94	2.20	4.14	4.98	5.64	10.62
	360	2.71	2.86	5.57	4.88	5.15	10.04
	400	3.81	3.83	7.64	5.01	5.03	10.04
	440	5.11	5.07	10.18	5.11	4.56	9.67

Effect of Spacing between Impellers on Power Consumption

Disc turbines, $n=2$, $D=10.16\text{cm}$, $T=29.21\text{cm}$, $H=40.64\text{cm}$, $C/D=1.0$

S (cm)	Speed (rpm)	PA (watts)	PB (watts)	PT (watts)	Np A	Np B	Np Total
7.62	150	0.70	0.57	1.27	4.14	3.37	7.51
	180	1.08	1.07	2.15	3.69	3.66	7.36
	200	1.43	1.54	2.97	3.57	3.84	7.41
	220	1.84	2.16	4.00	3.45	4.05	7.49
	240	2.39	2.78	5.17	3.45	4.01	7.46
	260	3.00	3.43	6.43	3.41	3.89	7.30
10.16	150	0.70	0.61	1.31	4.14	3.61	7.74
	180	1.08	1.18	2.26	3.73	4.04	7.77
	200	1.43	1.61	3.04	3.57	4.02	7.58
	220	1.92	2.02	3.94	3.60	3.79	7.38
	240	2.45	2.75	5.20	3.54	3.96	7.51
	260	3.04	3.65	6.69	3.45	4.14	7.59
11.43	150	0.66	0.76	1.42	3.90	4.49	8.39
	180	1.20	1.34	2.54	4.12	4.58	8.69
	200	1.59	1.78	3.37	3.97	4.44	8.40
	220	2.10	2.38	4.48	3.93	4.46	8.39
	240	2.80	3.17	5.97	4.04	4.57	8.62
	260	3.57	3.92	7.49	4.05	4.45	8.50
17.78	150	0.83	0.82	1.65	4.91	4.85	9.75
	180	1.42	1.40	2.82	4.86	4.79	9.65
	200	1.88	1.96	3.84	4.69	4.89	9.58
	220	2.51	2.51	5.02	4.70	4.70	9.41
	240	3.26	3.40	6.66	4.71	4.92	9.63
	260	4.00	4.32	8.32	4.54	4.90	9.44
20.32	150	0.81	0.83	1.64	4.79	4.91	9.70
	180	1.44	1.36	2.80	4.93	4.65	9.58
	200	1.97	1.92	3.89	4.91	4.79	9.70
	220	2.50	2.49	4.99	4.68	4.67	9.35
	240	3.31	3.40	6.71	4.78	4.91	9.68
	260	4.21	4.30	8.51	4.77	4.88	9.65

**Power Drawn by Each Impeller
for Three Impeller Configuration**

Disc turbines, D=10.16cm, T=29.21cm, H=40.64cm, C/D=1.0, S/D=1.0								
Speed (rpm)	PA (watts)	PB (watts)	PC (watts)	PT (watts)	Np A	Np B	Np C	Np Total
150	0.64	0.45	0.58	1.67	3.78	2.66	3.43	9.87
170	0.87	0.65	0.72	2.24	3.53	2.64	2.92	9.14
190	1.25	0.81	1.16	3.22	3.64	2.39	3.37	9.40
210	1.62	1.01	1.61	4.24	3.49	2.18	3.47	9.13
230	2.22	1.30	2.20	5.72	3.64	2.13	3.61	9.38
250	2.77	1.54	2.68	6.98	3.54	1.97	3.42	8.91
Disc turbines, D=7.62cm, T=29.21cm, H=40.64cm, C/D=1.0, S/D=1.0								
200	0.40	0.26	0.25	0.91	4.20	2.73	2.63	9.56
220	0.57	0.28	0.42	1.27	4.50	2.21	3.32	10.03
240	0.73	0.32	0.63	1.68	4.44	1.95	3.83	10.22
260	0.83	0.58	0.73	2.14	4.02	2.77	3.49	10.24
280	1.00	0.70	1.01	2.71	3.83	2.68	3.87	10.38
300	1.22	0.85	1.15	3.22	3.80	2.65	3.58	10.06
320	1.46	1.02	1.39	3.87	3.75	2.62	3.57	9.93
340	1.70	1.28	1.81	4.79	3.64	2.74	3.89	10.25
360	2.10	1.41	1.99	5.50	3.78	2.55	3.59	9.91